Molecular Neurobiology
https://doi.org/10.1007/s12035-018-0913-3

Neural Crest Stem-Like Cells Non-genetically Induced from Human Gingiva-Derived Mesenchymal Stem Cells Promote Facial Nerve Regeneration in Rats

Qunzhou Zhang[1] · Phuong D. Nguyen[2] · Shihong Shi[1] · Justin C. Burrell[3] · Qilin Xu[1] · Kacy D. Cullen[3] · Anh D. Le[1,4]

Received: 25 October 2017 / Accepted: 15 January 2018

Abstract
Non-genetic induction of somatic cells into neural crest stem-like cells (NCSCs) is promising for potential cell-based therapies for post-traumatic peripheral nerve regeneration. Here, we report that human gingiva-derived mesenchymal stem cells (GMSCs) could be reproducibly and readily induced into NCSCs via non-genetic approaches. Compared to parental GMSCs, induced NCSC population had increased expression in NCSC-related genes and displayed robust differentiation into neuronal and Schwann-like cells. Knockdown of the expression of Yes-associated protein 1 (YAP1), a critical mechanosensor and mechanotransducer, attenuated the expression of NCSC-related genes; specific blocking of RhoA/ROCK activity and non-muscle myosin II (NM II)-dependent contraction suppressed YAP1 and NCSC-related genes and concurrently abolished neural spheroid formation in NCSCs. Using a rat model of facial nerve defect, implantation of NCSC-laden nerve conduits promoted functional regeneration of the injured nerve. These promising findings demonstrate that induced NCSCs derived from GMSCs represent an easily accessible and promising source of neural stem-like cells for peripheral nerve regeneration.

Keywords Neural crest stem cells · Gingiva-derived mesenchymal stem cells · YAP1 · RhoA/ROCK · Facial nerve regeneration

Introduction

There has been growing enthusiasm for the combinatorial use of stem cells and biomaterial scaffolds in tissue engineering and regenerative medicine (TE/RM) [1] to provide transplantable tissues and organs for unmet clinical needs [2, 3], including neural tissues [4–6]. The source of stem cells in TE/RM includes embryonic stem cells (ESCs), induced pluripotent stem cells (iPSCs), and adult stem cells such as neural stem (NSC) or progenitor cells (NPCs) and mesenchymal stem cells (MSCs) derived from different tissues [7–9]. However, use of ESCs encounters ethical issues, and generation of neural progenitor cells or neural lineages from iPSCs is time-consuming and rigged with safety concerns in clinical application [10]. MSCs can be differentiated into functional glial and neuronal cells; however, the induction efficiency is quite low and variable due to their inherent heterogeneity. Recently, adult NSCs or NPCs have been proposed as a promising cell source to facilitate nerve repair/regeneration; nevertheless, it remains difficult to expand and propagate them in multiple passages to meet the cell number for clinical use [11]. Other studies have shown that somatic cells, including fibroblasts and MSCs, could be converted into multipotent and expandable NSCs or NPCs by direct reprogramming with a combination of transcription factors [12–18]. Meanwhile, induced NSCs or NPCs could be generated from somatic cells by non-genetic approaches, e.g., a combination of small-molecule compounds or under specific culture conditions [19–21].

✉ Anh D. Le
Anh.Le@uphs.upenn.edu

1 Department of Oral and Maxillofacial Surgery and Pharmacology, University of Pennsylvania School of Dental Medicine, 240 South 40th Street, Philadelphia, PA 19104, USA

2 Division of Plastic and Reconstructive Surgery, University of Pennsylvania Perelman School of Medicine, 3401 Civic Center Blvd, Philadelphia, PA 19104, USA

3 Department of Neurosurgery, University of Pennsylvania Perelman School of Medicine, 3320 Smith Walk, Philadelphia, PA 19104, USA

4 Department of Oral and Maxillofacial Surgery, Penn Medicine Hospital of the University of Pennsylvania, Perelman Center for Advanced Medicine, 3400 Civic Center Blvd, Philadelphia, PA 19104, USA

Published online: 25 January 2018

During embryogenesis, neural crest (NC) forms transiently in the dorsal neural primordium and its migratory NC cells invade nearly all tissues, giving rise to not only classic neural cells, but also diverse non-neural cells [22, 23]. More importantly, post-migratory NC-derived tissues/organs, including oral mucosa/gingival lamina propria [24–27], contain a small population of stem cells of NC origin (NCSCs), including MSCs [22, 24]. After isolation and in vitro culture, these NCSCs could differentiate into classical NC cell lineages, such as neurons and Schwann cells, and various non-neural cells such as melanocytes, endoneural fibroblasts, a subpopulation of bone marrow and dental mesenchymal stem cells [22, 28–30]. In comparison to mesodermal-derived MSCs, these NC-derived MSCs constitutively express neural-progenitor cell markers, such as nestin and p75, and possess highly neurogenic differentiation potentials [27, 29]. Most recently, it has been shown that neural crest stem-like cells could be induced from human postnatal fibroblasts by direct reprogramming with a single transcription factor SOX10 [17] or FoxD3 [31]. Therefore, efficient isolation and enrichment of NCSCs from adult tissues, particularly from neural crest-derived craniofacial tissues [23, 32], may provide an important alternative cell source for bioengineering nerve tissues.

We have isolated a unique subpopulation of MSCs from human gingival tissue (GMSCs) [33] and our recent study has shown that human GMSCs can be easily induced into neural progenitor-like cells, which displayed better therapeutic effects in the repair/regeneration of peripheral nerve injuries (PNI) than the parental GMSCs [34]. Here, we demonstrated that neural progenitor-like cells induced from human GMSCs under defined culture conditions were endowed with neural crest stem-like cell (NCSC) properties, whereby the RhoA/ROCK activity-mediated non-muscle myosin II (NM II)-dependent contraction of the actomyosin cytoskeleton and YAP1 activation play a pivotal role in the process. Using a rat model of facial nerve transection injury, we showed that GMSC-derived NCSCs in combination with a nerve conduit showed better therapeutic effects on facial nerve regeneration and functional recovery than parental GMSCs. Our findings suggest that GMSCs of NC-origin possess the intrinsic propensity to be reprogrammed to early NCSC-like cells, thus representing an easily accessible source of neural stem-like cells for cell-based therapy of post-traumatic peripheral nerve repair/regeneration.

Materials and Methods

Animals

Female Sprague-Dawley rats weighing 200–250 g (6–8 weeks old) were obtained from Charles River Laboratories. All animal procedures were approved by the Institutional Animal Care and Use Committee (IACUC) of University of Pennsylvania. Rats were group-housed in polycarbonate cages (three animals per cage) in the animal facilities with controlled temperature (23 °C ± 2 °C), 40–65% of humidity and a 12-h light/dark cycle, fed with a standard laboratory diet, and allowed ad libitum access to drinking water.

Cell Culture

Gingival tissues were obtained as remnants of discarded tissues under the approved Institutional Review Board (IRB) protocol at University of Pennsylvania. The isolation and characterization of human gingival tissue-derived MSCs (GMSCs) were described previously [33]. Culture plates were precoated with poly-L-ornithine (15 μg/ml) and laminin (5 μg/ml) in PBS at 37 °C for 2 h [35–37]. For neural induction, adherent monolayer GMSCs were collected and seeded onto laminin/poly-L-ornithine (LN/PLO) precoated 6-well plates (5×10^5 cells/well) with neural culture medium, DMEM/F12: neurobasal medium (1:1) supplemented with N2 (100×) [38, 39], B27 (50×), 100 U/ml penicillin, 100 μg/ml streptomycin, 55 μM β-mercaptoethanol (β-ME) (all from Life Technologies), 20 ng/mL of epidermal growth factor (EGF), and 20 ng/mL of basic fibroblast growth factor (bFGF) (Peprotech) (Table 1). After culture for 3 days under this condition, GMSCs aggregated into spheroids. To passage the spheroid cells, spheroids were collected and completely dissociated into single cells using StemPro® Accutase® Cell Dissociation Reagent (Life Technologies) and the cell viability was determined by trypan blue staining. Dissociated cells were seeded onto polyornithine/laminin precoated dishes for serial passaging and culture under the same conditions.

Neural Differentiation of GMSCs and Induced NCSCs

GMSCs or induced NSCSs were seeded onto poly-D-lysine pre-coated 4-well slide chamber (2×10^4/well) and cultured for 14 days at 37 °C and 5% CO_2 under neuronal or Schwann cell differentiation conditions, while the media were changed every 3d. Neuronal induction media contains neurobasal medium supplemented with 1% N2 supplement, 5% FBS serum, 0.5 μM all-*trans*-retinoic acid, and 10 ng/mL of brain-derived neurotrophic factor (BDNF) [20]. Schwann cell induction media contains α-MEM supplemented with 10% FBS, 35 ng/ml all *trans*-retinoic acid (RA), 5 μM forskolin, 10 ng/ml basic fibroblast growth factor (bFGF), 5 ng/ml platelet-derived growth factor AA (PDGF-AA), and 200 ng/ml heregulin-β-1 (PeproTech) (Table 1) [40, 41].

siRNA Transfection

Human YAP1 siRNA (sc-38637), a pool of 3 target-specific 19-25 nt siRNA, and a nonspecific control siRNA (sc-36869)

Table 1 Compositions of different culture media

	Components	Working concentration	Catalog number	Vendors
GMSC culture media				
	α-MEM	90%	12561-056	Life Technologies
	Fetal bovine serum (FBS)	10%	SER-500	ZenBio, Inc.
	Penicillin/streptomycin (100×)	100 U/100 μg/mL	15140-122	Life Technologies
	β-mercaptomethanol (55 mM, ×1000)	55 μM	21985-023	Life Technologies
NCSC induction media				
	DMEM/F12 (1:1)	50%	11330-032	Life Technologies
	Neurolbasal® medium	50%	21103-049	Life Technologies
	Human bFGF	20 ng/mL	100-18C	PeproTech
	Human EGF	20 ng/mL	AF-100-15	PeproTech
	β-mercaptomethanol (55 mM, ×1000)	55 μM	21985-023	Life Technologies
	*N2 (100×)		17-502-048	Life Technologies
	*B27 (50×)		17-504-044	Life Technologies
	Penicillin/streptomycin (100×)	100 U/100 μg/mL	15140-122	Life Technologies
*N2 supplement	Human Transferrin (Holo)	1.0 mM		
	Recombinant Insulin	0.086 mM		
	Progesterone	0.002 mM		
	Putrescine	10.0 mM		
	Selenite	0.003 mM		
*B27 supplement	Biotin	Unknown		
	DL Alpha Tocopherol	Unknown		
	Acetate	Unknown		
	DL Alpha-Tocopherol,	Unknown		
	Vitamin A	Unknown		
	BSA	Unknown		
	Fatty acide free Fraction V	Unknown		
	Catalase	Unknown		
	Human Recombinant Insulin	Unknown		
	Human Transferrin	Unknown		
	Superoxide Dismutase	Unknown		
	Corticosterone	Unknown		
	D-Galactose	Unknown		
	Ethanolamine HCl	Unknown		
	Glutathione (reduced)	Unknown		
	L-Carnitine HCl	Unknown		
	Linoleic Acid	Unknown		
	Linolenic Acid	Unknown		
	Progesterone	Unknown		
	Putrescine 2HCl	Unknown		
	Sodium Selenite	Unknown		
	T3 (triodo-I-thyronine	Unknown		
Schwann cell induction media	α-MEM	90%	12561-056	Life Technologies
	FBS	10%	SER-500	Zenbio, Inc.
	All trans-retinoic acid (RA)	35 ng/mL	R2625	Sigma
	Forskolin	5 μM	11018	Cayman Chemical
	bFGF	10 ng/mL	100-18C	PeproTech
	PDGF-AA	5 ng/mL	100-13A	Peprotech
	β-heregulin	200 ng/mL	100-03	PeproTech
	Penn/Streptomycin	100 U/100 μg/mL	15140-122	Life Technologies
Neuronal induction media	Neurolbasal® medium	95%	21103-049	Life Technologies
	FBS	5%	SER-500	Zenbio, Inc.
	All trans-retinoic acid (RA)	0.5 μM	R2625	Sigma
	BDNF	10 ng/mL	450-02	PeproTech
	Penn/Streptomycin	100 U/100 μg/mL	15140-122	Life Technologies

were obtained from Santa Cruz. A total of 2 × 105 GMSC-derived NCSC-like cells were seeded into six-well plates and transfected with the control and YAP1 siRNA according to the siRNA transfection protocol provided by the manufacturer (Santa Cruz). After 48 h, whole cell lysates were prepared for further analysis.

Western Blot Analysis

Whole cell lysates were separated on polyacrylamide-SDS gel and electroblotted onto nitrocellulose membrane (BioRad, Hercules, CA, http://www.bio-rad.com) (Supplemental Experimental Procedures). After blocking with TBS/5% nonfat dry milk, the membrane was incubated with antibodies against Nestin (Millipore), FoxD3, Slug (Santa Cruz), YAP1, RhoA, Sox9, Twist1 and Snail1 (Cell Signaling Technology) followed by incubation with a horseradish peroxidase (HRP)-conjugated secondary antibody, and the signals were visualized by enhanced chemiluminescence detection (ECL) (Santa Cruz). The blots were also re-probed with a specific antibody against β-actin (Sigma).

Flow Cytometry

Human GMSCs cultured under regular condition or NCSC induction conditions were harvested and washed twice with PBS containing 2% heat-inactivated FBS and resuspended in cell staining buffer (BioLegend, San Diego, CA, USA) at a concentration of 10^7/ml, followed by incubation with FITC-conjugated antibodies for human CD29, CD44, CD73, CD90 or an isotype-matched mouse IgG control (BioLegend) at 4 °C for 30 min. For analysis of CD271/p75 expression, cells were fixed in 2% paraformaldehyde (PFA) at 4 °C for 20 min. Then cells were washed and incubated with a rabbit anti-human p75 antibody (1:200; Bio-Rad) at 4 °C for 30 min, followed by incubation with FITC-conjugated goat anti-rabbit IgG (1:200) at 4 °C for 30 min. For analysis of the expression of NCSC-related transcriptional factors, SLUG, SOX9 and FOXD3, cells were immunostained by using the True-Nuclear™ Transcription Factor Buffer Set according to the manufacture's protocols (BioLegend). After staining, cells were washed twice with PBS/2% FBS and submitted to flow cytometric analysis (BD LSRII).

Immunofluorescence Studies

Cells fixed with 4% paraformaldehyde (PFA) were blocked and permeabilized for 1 h at room temperature in PBS with 2.5% goat serum and 0.5%Triton X-100, followed by incubation with the following primary antibodies at the appropriate dilution overnight at 4 °C: Nestin (mouse IgG, 1:250, MAB5326; Millipore), Sox9 (rabbit IgG, 1:250, CST), Snail1 (rabbit IgG, 1:250, CST), p75 (rabbit IgG, 1:250, Bio-Rad), FoxD3 (mouse IgG, 1:250; Santa Cruz), Slug (mouse IgG, 1:250, Santa Cruz), YAP1 (mouse IgG, 1:250, CST), CD29 (mouse IgG, 1:250, BD Bioscience), cleaved caspase-3 (Rabbit IgG, 1:250; Millipore), type I collagen (rabbit IgG, 1:250, Rockland Biotech). After washing with PBS, cells were incubated with appropriate secondary antibodies at room temperature for 1 h: goat anti-rabbit IgG–fluorescein isothiocyanate (FITC) (1:250, sc2012; Santa Cruz), goat anti-rabbit IgG–rhodamine (1:250, sc2091; Santa Cruz), goat anti-mouse IgG–FITC (1:250, sc-2010; Santa Cruz), goat anti-mouse IgG–rhodamine (1:250, sc2092; Santa Cruz). Isotype-matched control antibodies (BioLegend) were used as negative controls. Nuclei were counterstained with 4′, 6-diamidino-2-phenylindole (DAPI). Images were captured using Olympus inverted fluorescence microscope (IX73). For semi-quantitative analysis, cells with positive signals in at least six random high-power fields (HPF) were visualized, counted, and expressed as the percentage of total DAPI-positive cells [33].

Surgical Procedures

Adult Sprague-Dawley female rats (8 weeks old) were anesthetized intraperitoneally with ketamine/xylazine (100/10 mg/kg). Following sterile surgical technique, a preauricular incision with a marginal mandibular extension was made in the left face of the rat. Under a surgical microscope, buccal and marginal mandibular branches of the facial nerves were exposed and a 6-mm gap was created with a sharp microsurgical scissor at sites that were 10 mm distal to the stylomastoid foramen. The facial nerve gaps were bridged with AxoGuard® Neural Wrap Conduit (1.5 mm in diameter) (Cook Medical Inc., Bloomington, IN) in combination with GMSCs or induced NCSCs. Two 8/ Ethilon interrupted sutures were applied at each side of the gap. To apply GMSCs and induced NCSCs, cells (0.5×10^6/rat) were mixed with 30 μl of Matrigel and injected into AxoGuard Neural Wrap Conduit immediately following suture, while AxoGuard Neural Wrap Conduit filled with Matrigel alone were used as controls. To block the signal to the whisker pad, a 6-mm defect was created in the marginal mandibular branch and ligated with 8/0 Ethilon interrupted sutures. The muscle layers and skin were closed in a layered fashion [42–44].

Histological and Immunohistochemical Studies

The facial nerves were fixed in 4% PFA for 24 h and cryoprotected in 10, 20, and 30% sucrose and embedded in O.C.T. and 8 μm-thick cryostat sections were cut. After blocking and permeabilization in PBS with 3% bovine serum

albumin (BSA) and 0.5%Triton X-100 at room temperature for 1 h, the sections were incubated with primary antibodies for β-tubulin III (1:250) or S-100β (1:250) overnight at 4 °C, followed by incubation with FITC-conjugated secondary antibodies for 1 h at room temperature. Isotype-matched control antibodies (BioLegend) were used as negative controls. Nuclei were counterstained with DAPI.

Morphological Evaluation of Regenerative Nerves

Twelve weeks after surgery, the facial nerve segments covering the resected area were isolated and fixed with 2.5% glutaraldehyde overnight at 4 °C, and then postfixed with 1% osmium tetroxide (OsO4) for 2 h, dehydrated, and embedded in epoxy resin. Semi-thin sections (1-μm) were cut vertically with an ultramicrotome (EM UC7i, Leica Microsystems, Denver, CO, http://www.leica-microsystems.com), stained with 1% toluidine blue solution, and examined under a light microscope (Olympus IX-73). The density of the myelinated fibers (fibers/1000 μm^2) was analyzed from six nonverlapping visual fields per specimen. Ultra-thin sections (60 nm) were stained with lead citrate and uranyl acetate and then examined under a transmission electron microscope (TEM; JEM-1400; JEOL, Tokyo, Japan, http://www.jeol.co.jp). The diameter of myelinated fibers and axons and the thickness of the regenerated myelin sheath were evaluated by cellSens Dimension software (Olympus), and the G-ratio was calculated as the ratio of the inner axonal diameter to the total outer diameter of the fiber.

Facial Functional Analysis Using the Facial Palsy Score

Facial palsy scores were blindly evaluated from animals in different treatment groups at every week until the termination of the study according to the standards as described previously [43]. The facial palsy score was valued based on the following functional evaluation: (1) symmetry of the vibrissae at rest (0, asymmetry; 0.5, slightly; 1, normal); (2) motion of the vibrissae (0, no motion; 1, minor trembling; 2, effective movement; 3, normal); (3) symmetry of the nose at rest (0, asymmetry; 0.5, slightly; 1, normal); (4) motion of the nose (0, asymmetry; 1, slightly; 2, normal). A maximum seven-point indicates a normal midface without facial palsy, while a zero-point indicates complete facial palsy of the midface [43].

Compound Muscle Action Potential (CMAP) Recordings of the Vibrissa Muscles

CMAP of the regenerated facial nerve (left side) and the contralateral normal nerve (right side) was measured as described previously [43]. Following anesthesia, CMAP amplitude was recorded and calculated as a difference in voltage between the maximum and baseline CMAP amplitude. CMAP duration was calculated as the time between 2 points where the baseline is crossed by the rising and declining CMAP curves. CMAP latency was estimated as the time between the stimulus artifact and the point where the baseline was crossed by rising CMAP curve. CMAP recovery (%) = CMAP of regenerated facial nerve/CMAP of the contralateral nerve.

Statistical Analysis

All statistical analyses were carried out using *SPSS Statistics version 18.0* (IBM, Inc., Armonk, NY, USA). Direct comparisons between experimental and control groups were analyzed by paired Student's *t* test. One-way analysis of variance (ANOVA) was employed for multiple comparisons. Post-hoc pairwise comparison between individual groups was performed using the Tukey's test. All data were expressed as mean ± standard deviation (S.D.). A *P* value of less than 0.05 was considered statistically significant.

Results

Enriched Expressions of NCSC-Related Genes in GMSCs Cultured on Lamin/Poly-L-ornithine Pre-coated Dishes with Defined Neural Progenitor Cell Culture Medium

We initially seeded GMSCs into tissue culture dishes pre-coated with either laminin or poly-L-ornithine (PLO) or both (LN/PLO) in complete neural progenitor cell culture medium [35, 36] for 3 days. Morphologically, GMSCs cultured under PLO- or LN/PLO-coating conditions spontaneously aggregated into 3D-spheroid structures, while spheroid formation was less efficient with PLO or LN alone than LN/PLO coating (Fig. 1a). The PLO, LN and LN/PLO substrates induced protein expression of several neural crest stem cell (NCSC)-related genes, including NESTIN, FOXD3, SOX9, SLUG, SNAIL1, and TWIST1 [22, 31, 45, 46], whereas LN/PLO had a stronger effect than PLO or LN alone (Fig. 1b). Even though SOX10 is well accepted as one of the classical NCSC-related transcription factors in mouse embryonic and adult neural crest cells, it is not consistently expressed in human adult NCSCs [22, 29, 30]. Similarly, we did not observe a consistent change in the expression of SOX10 in human GMSCs under our current experimental conditions (data not shown). The LN/PLO substrate induced morphological changes in a gradual fashion with a more discernible spheroid structure on day 3 (Fig. 1c); the spheroid formation appeared to correlate with an increased expression of NCSC-related genes, as early as 4 h, under LN/PLO-coating conditions (Fig. 1d), and sustained at a relatively high level up to 3 days of the course of the study (Fig. 1d, e).

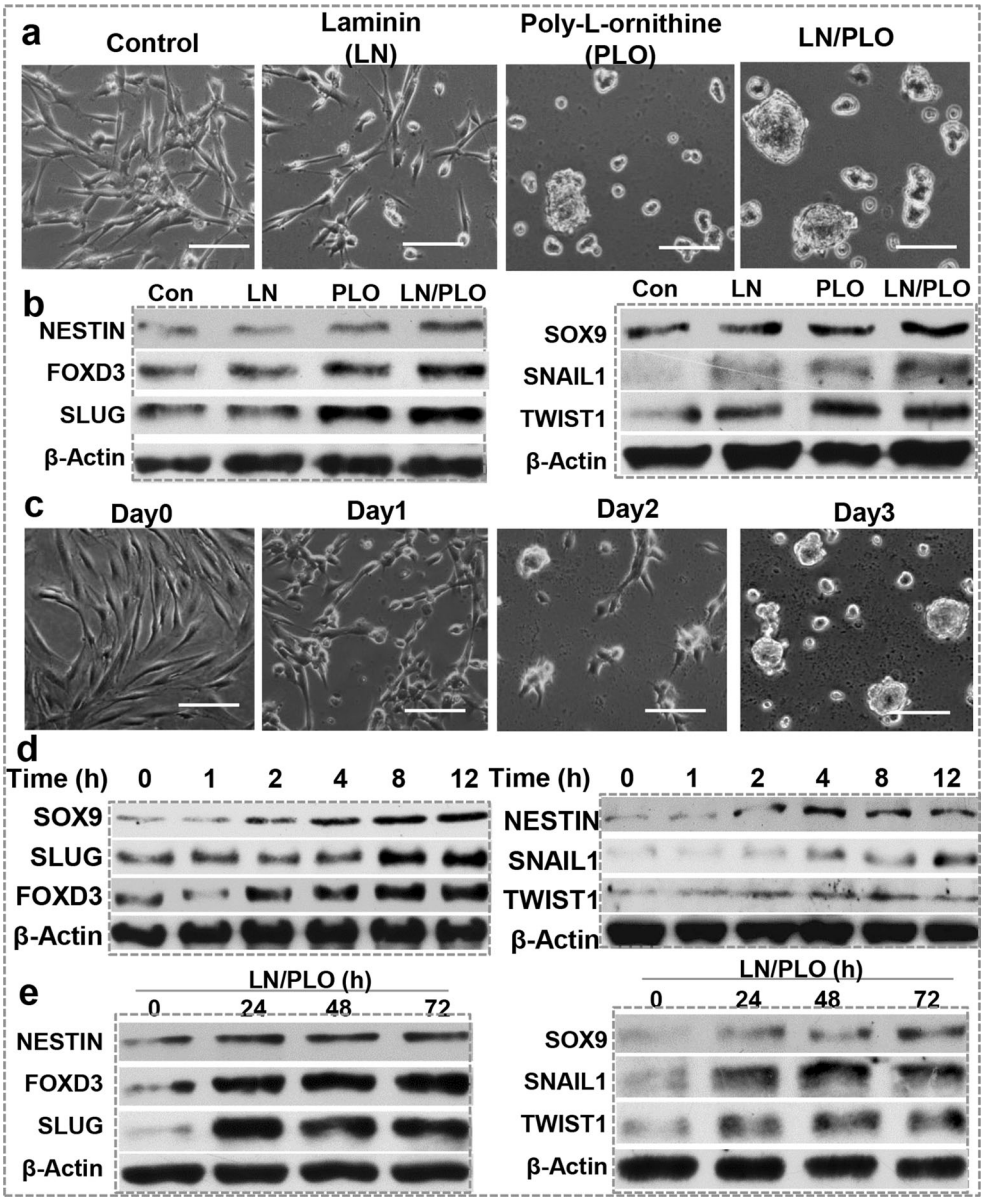

Fig. 1 Increased expression of NCSC-related genes in human GMSCs under defined culture conditions. **a** Morphological changes in GMSCs after culturing for 3 days on laminin/poly-L-ornithine (LN/PLO)-precoated plates with defined neural culture medium, DMEM/F12: neurobasal medium (1:1) containing N2, B27, 20 ng/mL EGF and 20 ng/mL bFGF. **b** Western blot data showed increased expression of NCSC-related genes, including NESTIN, FOXD3, SOX9, SLUG, SNAIL1, and TWIST1, in GMSCs cultured for 3 days on culture plates pre-coated with either laminin (LN), poly-L-ornithine (PLO) or both (LN/PLO), while cells cultured on non-coated culture plates with defined neural culture medium were used as controls (Con). **c** Dynamic morphological changes in GMSCs following culturing on LN/PLO-precoated culture plates with defined neural culture medium for different days. **d**, **e** Time-course studies on the expression of NCSC-related genes in human GMSCs following culturing on LN/PLO pre-coated culture plates with defined neural culture medium for different time periods as determined by Western blot. β-actin served as the internal reference. Scale bar: 200 μm. Data are representative of 3 independent experiments

To further characterize GMSC-derived spheroids, we dissociated them into single cells and continue similar neural culture conditions for 6 days (Fig. 2a). The induced neural progenitor-like cells (NCSC) formed compact colonies and showed marked increase in protein expression of NCSC-related genes as compared with non-induced parental GMSCs (Fig. 2b). Immunofluorescence studies further confirmed a significant increase in the percentage of cells that were positively stained for NCSC-related markers, NESTIN, $p75^{NTR}$, SOX9, FOXD3 (Fig. 2c–e), SLUG, and SNAIL1 (Fig. 2f–h).

Increased Expression of NCSC-Related Genes in GMSCs in Sphere-Forming Culture

The suspension sphere-forming culture approach is commonly used to enrich and isolate NCSCs from a variety of adult tissues [25, 47, 48]. We next characterize the expression of NCSC-related markers by GMSCs under sphere-forming culture conditions (Fig. 3a). We observed a gradual increase in protein expression of NCSC-related genes in GMSCs under sphere-forming condition, as compared to those under adherent condition, in a time-dependent manner, which peaked at day 3 (Fig. 3b). The increased expression of these NCSC-related genes was also observed in the third passage of spheroid GMSCs (Fig. 3c). Immunofluorescence studies further confirmed a significant enrichment of cells that positively expressed NCSC-related genes in spheroid culture (Fig. 3d–h); approximately 40% of cells within spheroids were positive for BrdU and expressed PCNA (Fig. 3i). These findings suggest that sphere-forming culture can facilitate the induction of GMSCs into NCSC-like cells.

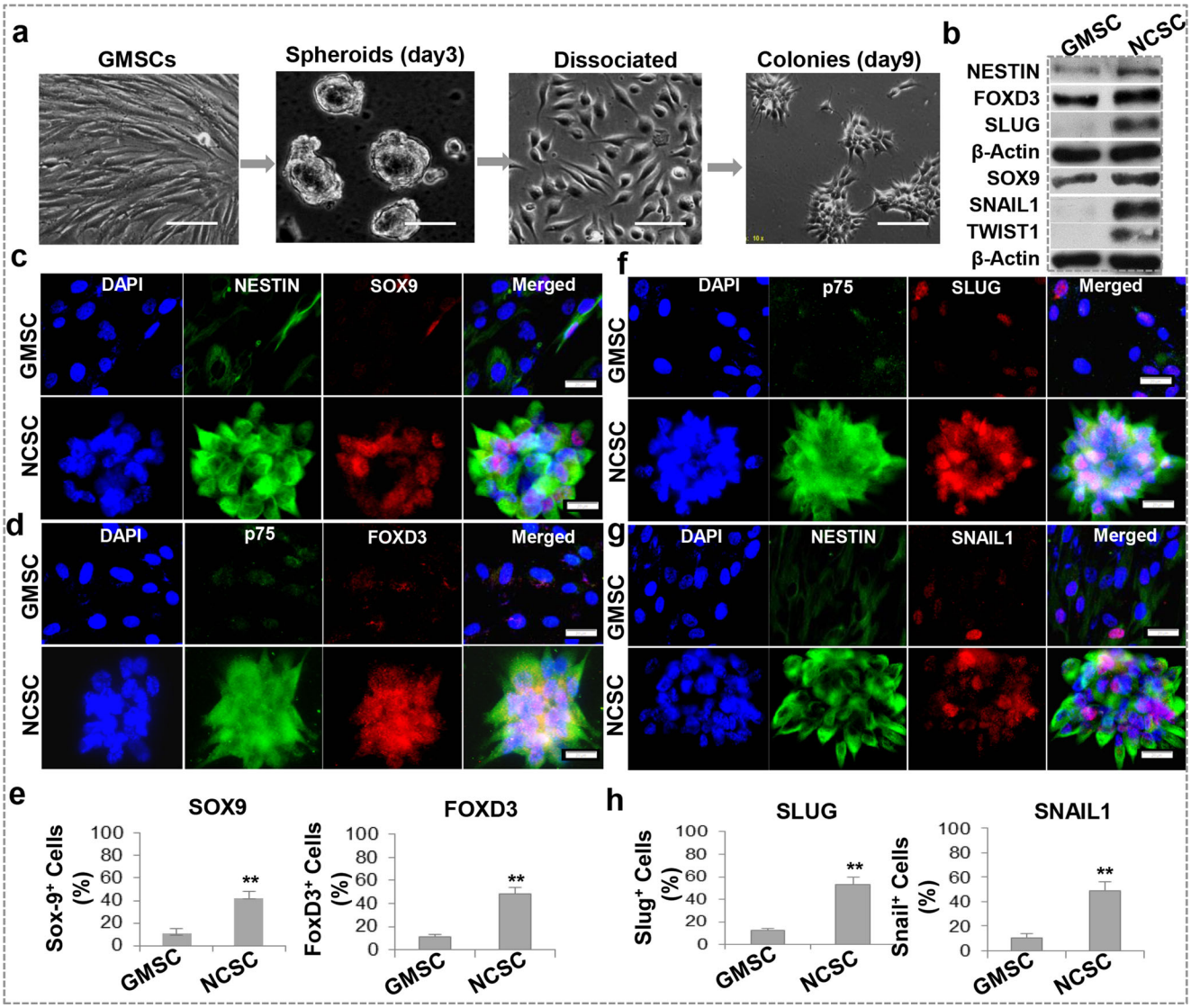

Fig. 2 Induction of NCSCs from human GMSCs under defined culture conditions. **a** Morphology of NCSC-like colonies induced from GMSCs after culturing for 9 days on LN/PLO-precoated plates with DMEM/F12: neurobasal medium (1:1) containing N2, B27, 20 ng/mL EGF and 20 ng/mL bFGF. Scale bar: 200 μm. **b** Western blot analysis showed increased expression of NCSC-related genes, including NESTIN, FOXD3, SOX9, SLUG, SNAIL1, and TWIST1, in induced NCSC-like colonies as compared to non-induced GMSCs. β-actin served as the internal reference. **c**–**e** Immunocytochemistry and semi-quantification showed increased expression of NCSC-related genes, SOX9 and FOXD3, in induced NCSC-like colonies as compared to non-induced GMSCs. **f**–**h** Immunocytochemistry and semi-quantification showed increased expression of NCSC-related genes, SLUG and SNAIL, in induced NCSC-like colonies as compared to non-induced GMSCs. Cell nuclei were counter-stained by DAPI (blue). Scale bar: 20 μm. Data are representative of 3 independent experiments. $^{**}P < 0.01$ versus the control GMSCs

Optimizing the Induction of NCSC-Like Cells from GMSCs

Previous studies showed that combination of chemically defined medium using small-molecule inhibitors of glycogen synthase kinase 3 (GSK-3β) activity and TGF-β signaling pathways could optimize the induction of human neural crest cells [49]. Following culture under LN/PLO-coating culture conditions for 3 days, GMSCs were passaged and treated with CHIR99021 (2.5 μM), a potent and specific inhibitor of GSK-3β, or SB43152 (5 μM), a potent and selective TGF-β type I receptor activin receptor-like kinase (ALK5), or both (Fig. 4a, b). Our results showed that addition of CHIR99021 and SB43152 synergistically increased the expression of FOXD3, SLUG, and SOX9 proteins in GMSC-derived NCSCs (Fig. 4c).

We then observed the dynamic changes in the expression of a panel of mesenchymal stromal cell (MSC)-associated cell surface markers, including CD29, CD44, CD73, and CD90, in GMSCs under the defined induction conditions with CHIR99021 and SB43152 at different passages (Fig. 4a). Morphologically, induced GMSCs became more homogeneous and epithelial-like cells (Fig. 5a); the expression of

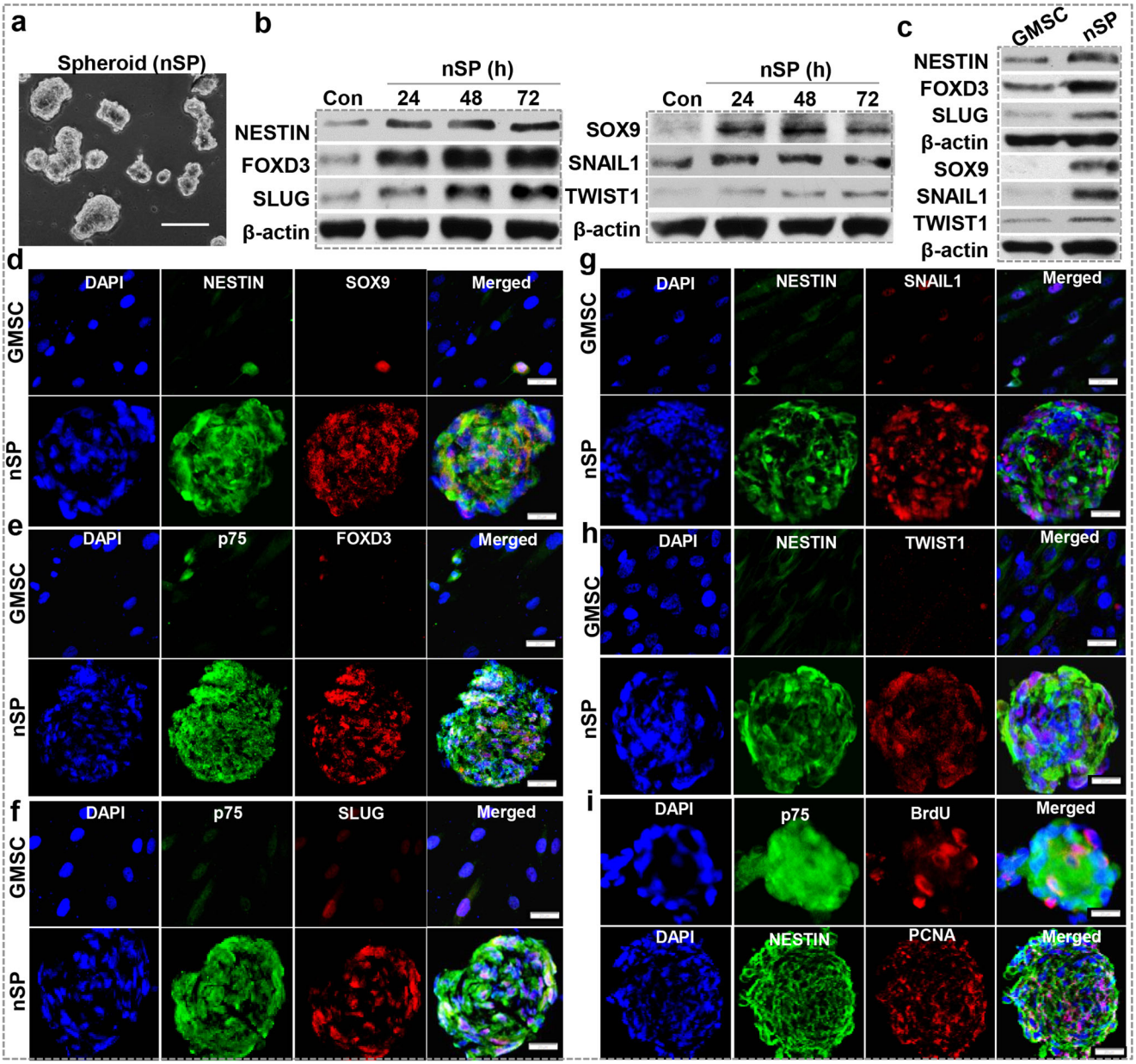

Fig. 3 Sphere-forming culture induced the expression NCSC-related genes in human GMSCs. **a** GMSCs aggregated into 3D-spheroids after culturing for 48 h in ultra-low attachment plates with defined neural culture medium, DMEM/F12: neurobasal medium (1:1) containing N2, B27, 20 ng/mL EGF and 20 ng/mL bFGF. Scale bar: 200 μm. **b** Western blot analysis showed increased expression of NCSC-related genes, including NESTIN, FOXD3, SOX9, SLUG, SNAIL1, and TWIST1, in GMSCs following sphere culturing (nSP) for different time periods. **c** Increased expression of NCSC-related genes in the third passage of spheroid GMSCs as compared to adherent GMSCs as determined by Western blot. β-actin served as the internal reference. **d**–**h** Immunocytochemistry showed increased expression of NCSC-related genes in spheroid GMSCs as compared to adherent GMSCs. **i** Immunocytochemistry showed that about ~40% of cells inside the spheroid were positively BrdU-labeled and express proliferating cell nuclear antigen (PCNA). Cell nuclei were counter-stained by DAPI (blue). Scale bar: 20 μm. Data are representative of 3 independent experiments

CD90 and CD44 dramatically decreased as early as day 3, while the expression of CD29 and CD73 also gradually decreased (Fig. 5b). Interestingly, the expression of CD271/p75, a classical neural crest marker, gradually increased following spheroid induction (Fig. 5c). Likewise, a consistent increase in the expression of NCSC-related transcription factors, SLUG, SOX9, and FOXD3, was observed in GMSCs following induction for up to 12 days with three consecutive passages as determined by immunofluorescence staining, flow cytometry, and Western blot (Fig. 6a–c), respectively.

We next determined the multipotent neural differentiation capabilities of GMSC-derived NCSCs. Upon exposure to neuronal or Schwann cell differentiation conditions for 14 days, about 20% of parental GMSCs could differentiate into

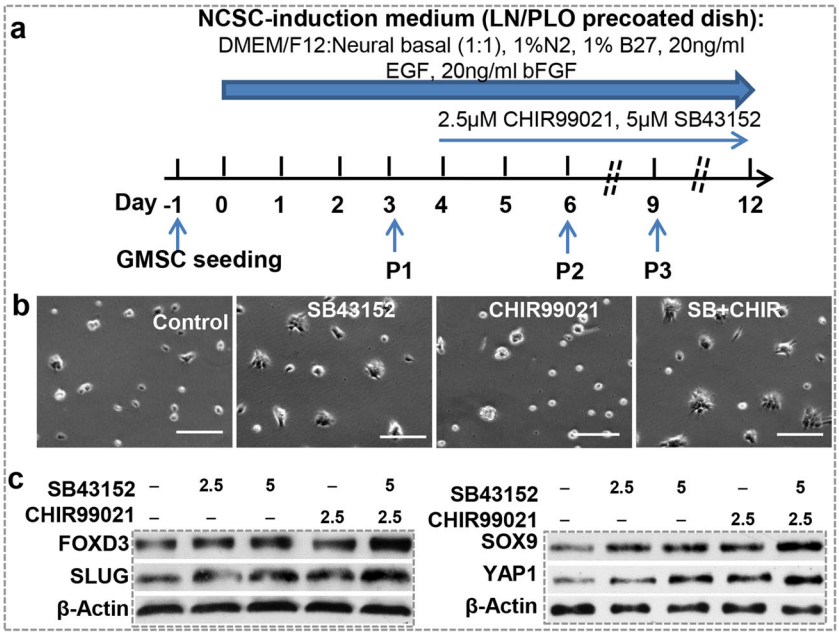

Fig. 4 Blocking GSK-3β activity and TGF-β signaling pathways enhanced the expression of NCSC-related genes in human GMSCs under defined culture conditions. **a** Protocol for the induction of NCSCs from GMSCs. GMSCs were seeded onto LN/PLO-precoated culture plates and cultured with regular medium (α-MEM with 10% FBS and antibiotics) for 24 h. On the second day (day 0), the medium was replaced with the defined NCSC-induction media, DMEM/F12: neurobasal medium (1:1) containing N2, B27, 20 ng/mL EGF and 20 ng/mL bFGF. On day 3, cells were passaged and continuously cultured under the same condition; whereas starting on day 4, 2.5 μM CHIR99021 and 5 μM SB43152 were included in the induction medium. Cells were continuously cultured and passaged under the same condition for up to 12 days. **b** After the addition of 2.5 μM CHIR99021 and 5 μM SB43152 for 48 h (day 6), cells were observed under a microscope. Scale bar: 100 μm. **c** On day 6, after the addition of CHIR99021 and SB43152 for 48 h, cells were harvested and the protein expression of FOXD3, SLUG, SOX9, and YAP1 was determined by Western blot analysis. β-actin served as the internal reference. Data are representative of 3 independent experiments

S-100β$^+$ Schwann cells or β-tubulin III$^+$ neuronal cells, whereas more than 80% of GMSC-derived NCSCs could differentiate into neuronal and Schwann-like cells (Fig. 6d, e). Taken together, our findings suggest that GMSCs can be directly and robustly reprogrammed into NCSC-like cells under defined serum-free culture conditions.

Potential Role of YAP1 in the Induction of NCSC-Like Cells from GMSCs

Previous studies have indicated that Yes-associated protein (YAP) signaling plays an important role in mechanotransduction sensing [50], regulation of the proliferation, expansion, and activation of neural progenitor or neural stem cells [51, 52], and human neural crest cell fate and migration [53]. We then determined whether YAP1 signaling was involved in the induction of NCSC-like cells from GMSCs. Our results showed that GMSCs cultured for 24 h on culture dishes precoated with poly-L-ornithine (PLO) alone or in combination with laminin (LN), but not with laminin alone, showed a robust increase in the expression of YAP1 (Fig. 7a). YAP1 level gradually increased in GMSCs as early as 2 h following culture on LN/PLO-precoated plates in defined neural culture medium (Fig. 7b), and maintained at a high level for up to 72 h (Fig. 7c). As expected, LN/PLO coating had minimal effects on the expression level of TAZ and phosphorylated YAP (Ser^{127}), the inactive form of YAP (Fig. 7a–c). Both Western blot and immunofluorescence studies showed that NCSC-like cells expressed a higher level of YAP1 than the parental GMSCs (Fig. 7d–f). Under sphere-forming culture condition, YAP1 expression also significantly increased in spheroid GMSCs as compared to adherent GMSCs (Fig. 7g, h). Knockdown of YAP1 expression in NCSC-like cells significantly downregulated the expression of several NCSC-related genes (Fig. 7i). Our results also showed that addition of CHIR99021 and SB43152 could synergistically increase the expression of YAP1 under the defined induction conditions (Fig. 4c). These findings suggest that YAP signaling may play an important role in orchestrating the induction of NCSC-like cells from GMSCs.

RhoA Activity-Mediated Non-muscle Myosin II (NM II) -Dependent Contraction of the Actomyosin Cytoskeleton Contributes to Induction of NCSC-Like Cells from GMSCs

It has been reported that actomyosin cytoskeleton is essential in mechanical signal transduction and that coactivators YAP and TAZ serve as the downstream mediators or

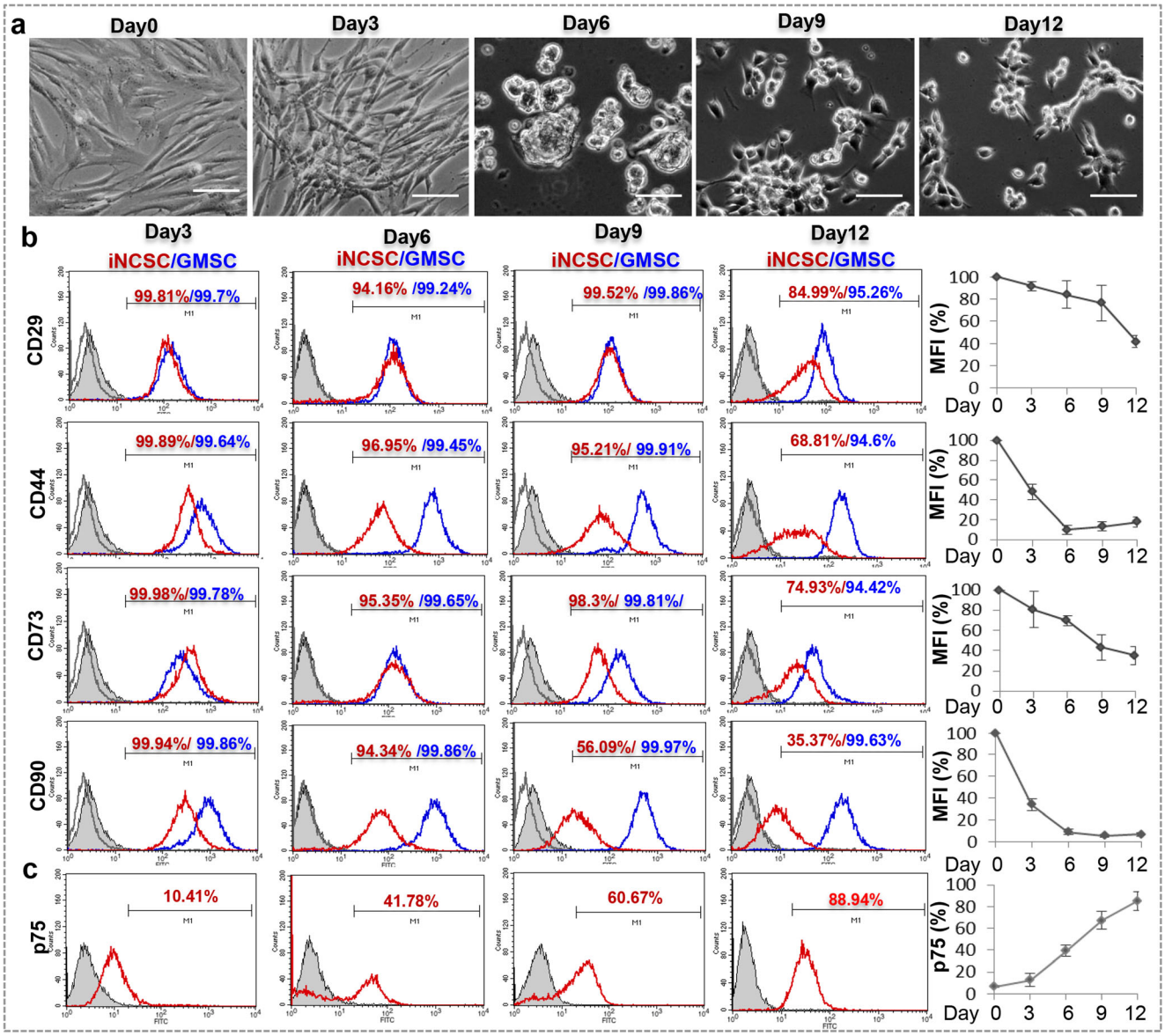

Fig. 5 Dynamic changes in the expression of markers for mesenchymal stromal cells and NCSCs in human GMSCs under defined culture conditions. **a** GMSCs underwent morphological changes following culture and serial passaging for different time periods on LN/PLO-precoated plates with DMEM/F12: neurobasal medium (1:1) containing N2, B27, 20 ng/mL EGF, 20 ng/mL bFGF. Starting from day 4, CHIR99021 (2.5 μM) and SB43152 (5 μM) were included in the induction medium. Scale bar: 200 μm. **b** Loss of the expression of mesenchymal stromal cell markers CD29, CD44, CD73, and CD90 on GMSCs following culture under defined NCSC-induction conditions for different time periods as determined by flow cytometric analysis. Blue histograms represent GMSCs and the red histograms represent induced (NCSC). MFI, mean fluorescence intensity. **c** Increasing expression of a classical neural crest cell marker, CD271/p75, on GMSCs following culture under defined NCSC-induction conditions for different time periods as determined by flow cytometric analysis. Data are representative of 3 independent experiments

effectors of mechanical cues [50]. We next determined whether Rho-associated kinase (ROCK)-mediated non-muscle myosin II (NM II)-dependent contraction of the actomyosin cytoskeleton [54, 55] was involved in the induction of GMSCs into NCSC-like cells. To this purpose, GMSCs were cultured under NCSC induction conditions in the absence or presence of (±)-blebbistatin, a specific inhibitor of NMII activity [56], and Y27632, a specific ROCK activity inhibitor [54] for 24–72 h, while (+)-blebbistatin, an inactive enantiomer of (±)-blebbistatin served as a control. Our results showed that inhibition of NMII and ROCK activities prevented GMSCs, cultured on LN/PLO pre-coated dishes, from aggregating into spheroids (Fig. 8a). Next, we determined whether the change in RhoA expression affected GMSCs undergoing NCSC induction. Our data showed that RhoA expression time-dependently increased in GMSCs under both LN/PLO-coating and sphere-forming culture conditions (Fig. 7a; Fig. 8b).

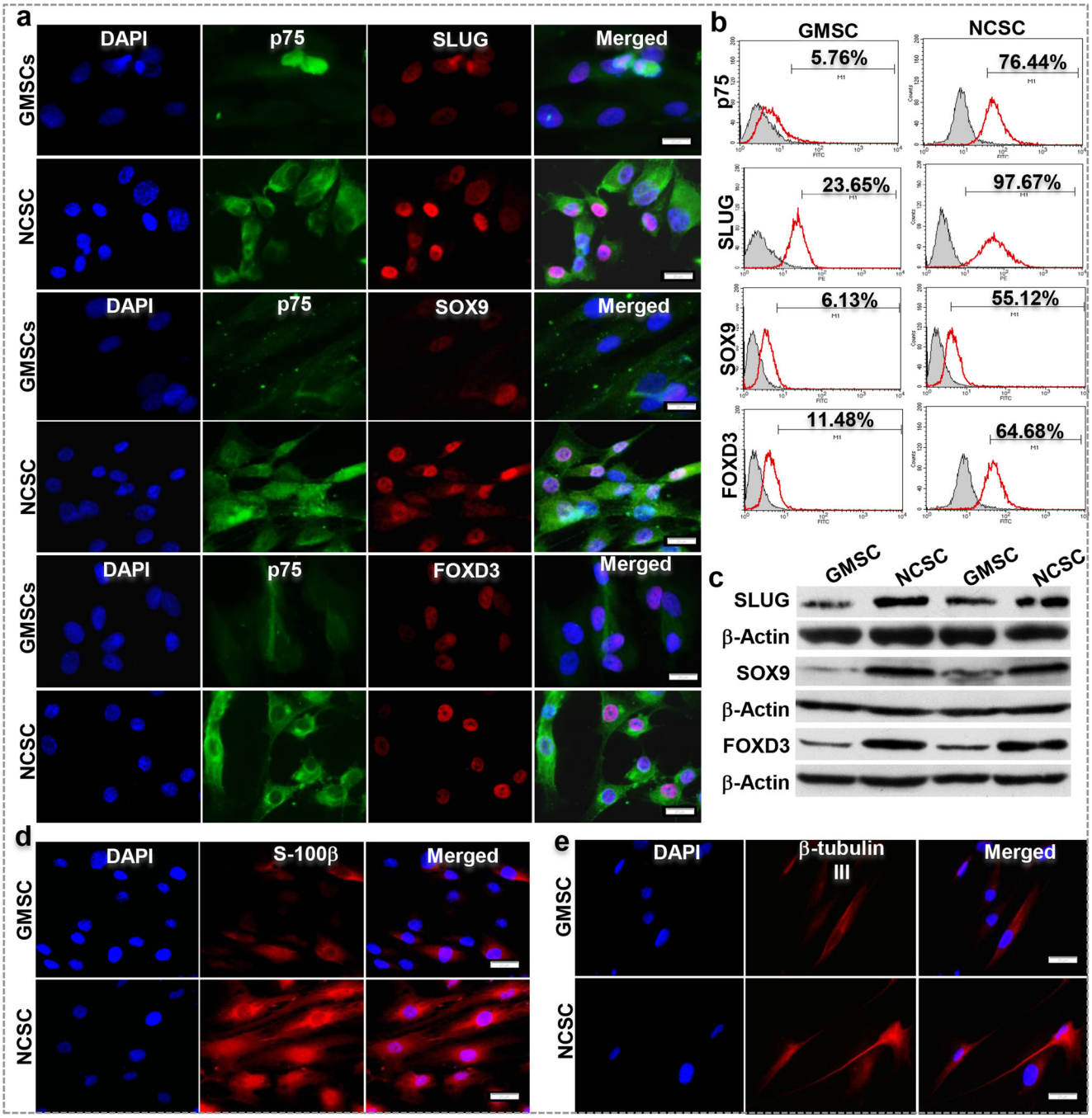

Fig. 6 Characterization of NCSCs induced from human GMSCs. GMSCs were seeded into LN/PLO-precoated plates, cultured and serially passaged under defined induction media, DMEM/F12: neurobasal medium (1:1) containing N2, B27, 20 ng/mL EGF and 20 ng/mL bFGF. Starting from day 4, CHIR99021 (2.5 μM) and SB43152 (5 μM) were included in the induction media. At day 12, cells were collected for further analysis. **a** Immunofluorescence study on the expression of p75, SLUG, SOX9, and FOXD3 protein in induced NCSCs as compared with GMSCs. Cell nuclei were counter-stained by DAPI (blue). Scale bar: 20 μm. **b** Flow cytometric analysis of the expression of p75, SLUG, SOX9, and FOXD3 protein in induced NCSCs as compared with GMSCs. **c** Western blot analysis of the expression of p75, SLUG, SOX9, and FOXD3 protein in induced NCSCs as compared with GMSCs. β-actin served as the internal reference. **d** GMSCs and their derivative NCSC-like cells were seeded onto poly-D-lysine pre-coated 4-well chamber slides and cultured under Schwann cell induction conditions for 14 days. The expression of S-100β was determined by immunocytochemistry. **e** GMSCs and their derivative NCSC-like cells were seeded onto poly-D-lysine pre-coated 4-well chamber slides and cultured under neuronal cell induction conditions for 14 days. The expression of β-tubulin III was determined by immunocytochemistry. Cell nuclei were counter-stained by DAPI (blue). Scale bar: 20 μm. Data are representative of 3 independent experiments

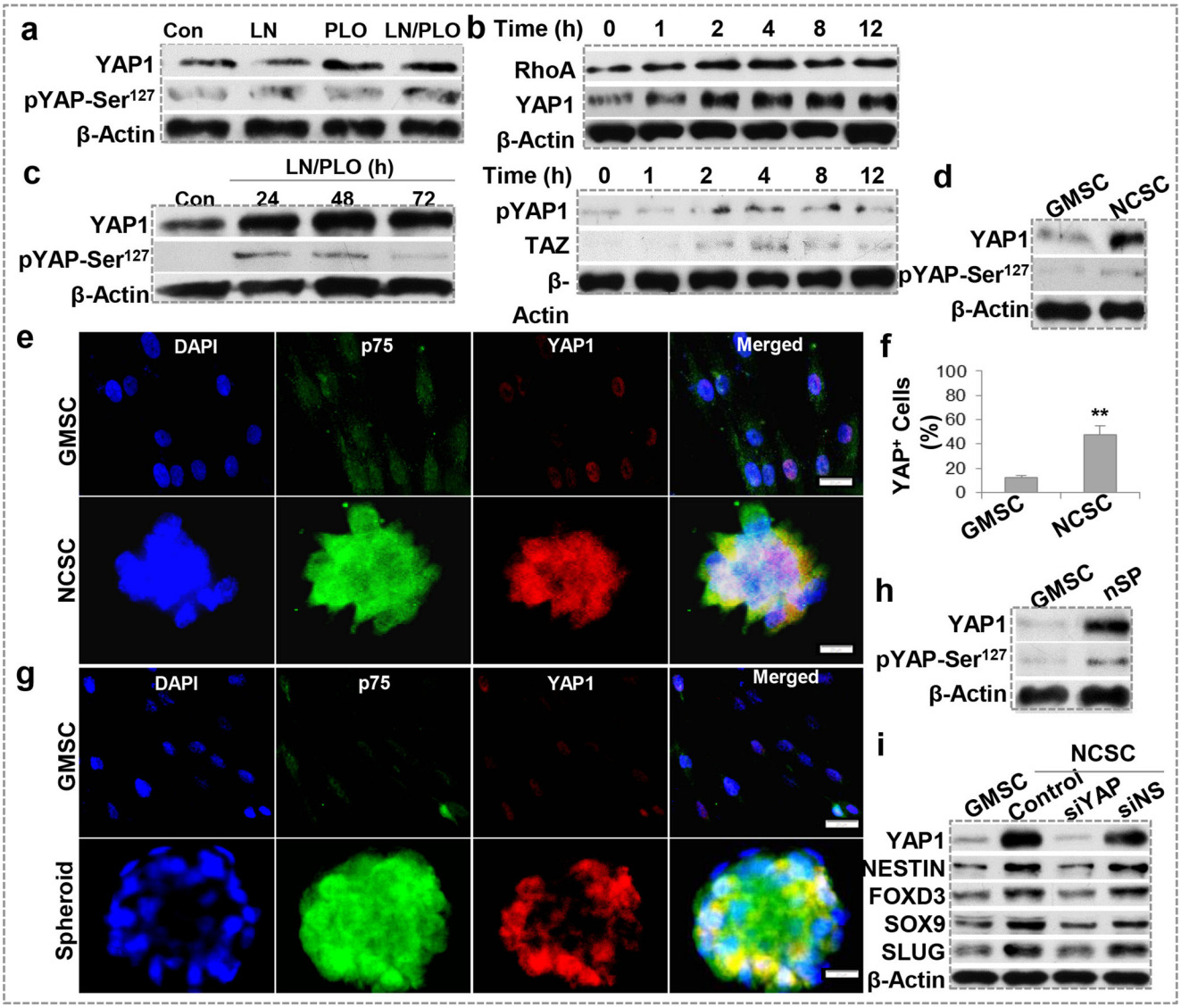

Fig. 7 Increased expression of YAP1 in human GMSCs under NCSC-induction conditions. **a** GMSCs were seeded into culture dishes pre-coated with either laminin (LN), poly-L-ornithine (PLO), or both (LN/PLO) and cultured for 24 h with defined NCSC-induction media, DMEM/F12: neurobasal medium (1:1) containing N2, B27, 20 ng/mL EGF and 20 ng/mL bFGF. The expression of YAP1 and phosphorylated YAP1 (pYAP-Ser^{127}) was determined by Western blot. **b**, **c** Time course studies on the expression of RhoA, YAP1, pYAP-Ser^{127}, and TAZ in GMSCs cultured in LN/PLO-precoated plates with the defined induction medium for different time periods as determined by Western blot. **d**–**f** Increased expression YAP1 in induced NCSC-like colonies (NCSCs) in comparison to non-induced GMSCs as determined by Western blot (**d**) and immunocytochemistry (**e**, **f**), respectively. **g**, **h** Increased expression YAP1 in spheroid GMSCs in comparison to that in their adherent counterparts as determined by immunocytochemistry (**g**) and Western blot (**h**), respectively. Cell nuclei were counter-stained by DAPI (blue) ($n = 5$). Scale bar: 20 μm. $^{**}P<0.01$ versus the control GMSCs. **i** Western blot analysis showed that knockdown of YAP1 expression by transfection with specific YAP1 siRNA (YAP-siR) significantly inhibited the expression of NCSC-related genes, including NESTIN, FOXD3, SOX9, and SLUG in NCSC-like cells induced from GMSCs, whereas a non-specific siRNA (NS-siR) was used as a control. β-actin served as the internal reference. Data are representative of 3 independent experiments

Subsequently, we determined the effect of blocking NMII and ROCK activity on the expression of NCSC-related genes and demonstrated that treatment with (±)-blebbistatin or Y27632, but not (+)-blebbistatin, led to a dose-dependent reduction in the expression of RhoA and YAP1 (Fig. 8c). Consistently, blocking NMII and ROCK activity robustly inhibited the expression of NCSC-related genes (Fig. 8c). Similarly, blocking the activities of NMII and RhoA significantly inhibited 3D-spheroid formation and the expression of YAP1 and NCSC-related genes, NESTIN, FOXD3, SOX9, SLUG, and SNAIL1, in GMSCs following culture for 3 days in ultra-low attachment plate with the defined NCSC-induction media (Fig. 8d, e). These findings suggest that RhoA/NMII/YAP1 axis-mediated biomechanical signal transduction may play an important role in the conversion of GMSCs into NCSC-like cells.

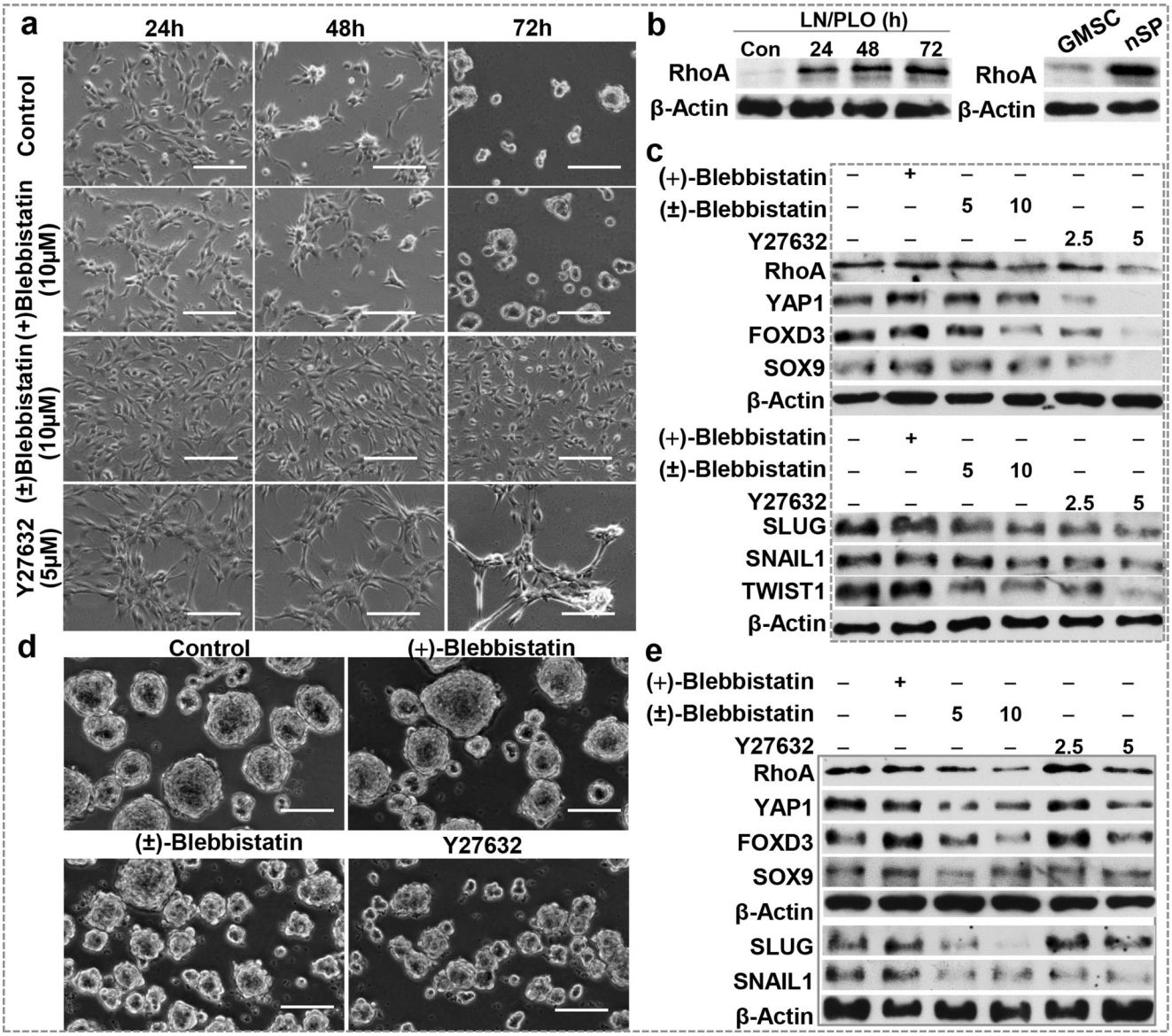

Fig. 8 Effects of blocking activities of non-muscle myosin II (NMII) and Rho A on the expression of NCSC-related genes. **a** Treatment with (±)-Blebbistatin (10 μM), a specific inhibitor of non-muscle myosin II activity, or Y27632 (5 μM), a specific inhibitor of RhoA/ROCk activity, prevented spheroid formation of GMSCs culturing on LN/PLO-precoated plates with defined induction media, DMEM/F12: neurobasal medium (1:1) containing N2, B27, 20 ng/mL EGF and 20 ng/mL bFGF, whereas (+)-Blebbistatin (10 μM), an inactive enantiomer of (±)-Blebbistatin, had no effects on spheroid formation of GMSCs. Scale bar: 200 μm. **b** Western blot showed that expression of RhoA was increased in GMSCs following culture on LN/PLO pre-coated plates for different time periods (the left panel) or under neurosphere culture condition for 48 h (the right panel) with defined NCSC-induction media. **c** Blocking the activities of non-muscle myosin II (NMII) and RhoA significantly inhibited the expression of YAP1 and NCSC-related genes, NESTIN, FOXD3, SOX9, SLUG and SNAIL1, in GMSCs following culture on LN/PLO pre-coated plates with the defined NCSC-induction media for 3 days. (**d, e**) Blocking the activities of non-muscle myosin II (NMII) and RhoA significantly inhibited 3D–spheroid formation and the expression of YAP1 and NCSC-related genes, NESTIN, FOXD3, SOX9, SLUG, and SNAIL1, in GMSCs following culture for 3 days in ultra-low attachment plate with the defined NCSC-induction media. β-actin served as the internal reference. Scale bar: 200 μm. Data are representative of 3 independent experiments

Transplantation of Nerve Conduits Laden with NCSC-Like Cells Promotes Rat Facial Nerve Regeneration

We next used a facial nerve transection model in rat to evaluate the nerve regenerative potentials of GMSC-derived NCSCs transplanted with nerve conduits. Twelve weeks after transplantation, continuity of the nerve was observed (Fig. 9a). Clinical nerve function assessment at several follow-up intervals, 4 to 12 weeks after surgery, indicated that both GMSC and NCSC groups showed significantly improved facial palsy scores as compared to the nerve conduit alone, whereas NCSC group demonstrated even higher scores than the GMSC group (Fig. 9b). Electrophysiological analysis

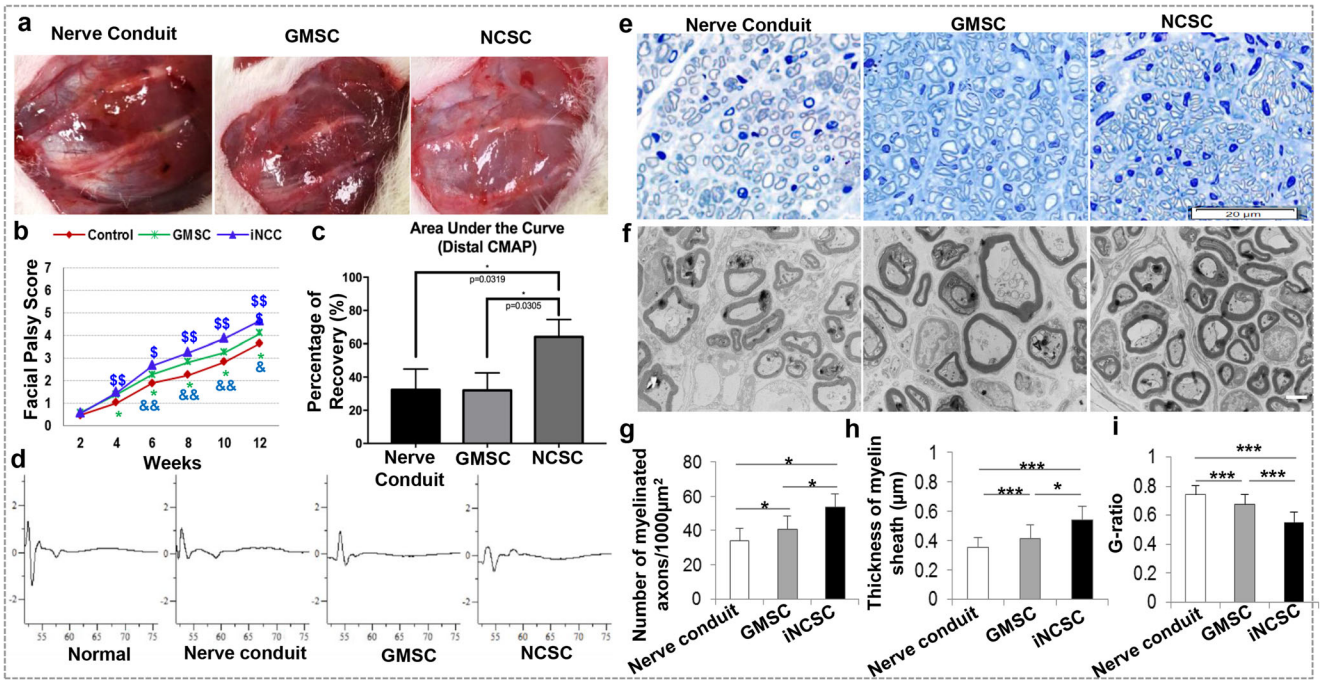

Fig. 9 Implantation of nerve conduits laden with human GMSC-derived NCSCs promotes regeneration of transected rat facial nerves. **a** Representative clinical photographs showing continuity of regenerated facial nerves at 12 weeks following implantation of a nerve conduit alone or in combination with GMSCs and NCSCs ($n = 5$). **b** Facial palsy scores evaluated at different time points following transplantation ($n = 5$). $^{*}P<0.05$, GMSC group v.s. nerve conduit alone; $^{\$}P < 0.05$, $^{\$\$}P < 0.01$, $^{\$\$\$}P < 0.001$, NCSC group v.s. nerve conduit alone; $^{\&}P < 0.05$, $^{\&\&}P < 0.01$, NCSC group *v.s.* GMSC group by Student's *t* test and 1-way ANOVA with Tukey's post hoc test. **c**, **d** Compound muscle action potential (CMAP) recordings of the vibrissal muscles of both the injury side and the normal side of rats ($n = 3$). $^{*}P<0.05$ by paired Student's *t* test. Data are representative of 2 independent experiments. **e** Toluidine blue staining of semi-thin sections of the middle segment of the regenerated nerve samples at 12 weeks after surgery. Scale bars, 20 μm. **f** Transmission electron microscopy (TEM) of ultrathin sections of the middle segment of the regenerated nerve samples at 12 weeks after surgery. Nerves from implantation of nerve conduit alone group showed poorly regenerated nerves composed of thin, dispersed myelinated and non-myelinated nerve fibers. On the contrary, combinatory implantation of nerve conduit and cells, particularly iNCSCs, showed well regenerated nerves composed of thick and ordered myelinated nerve fibers. Scale bars, 2 μm. Histograms show **g** density of myelinated axons (the number of myelinated axons/1000μm^2), **h** the thickness of the regenerated myelin sheaths, and **i** the G-ratios (the inner axonal diameter/the outer myelinated fiber diameter). Data are shown as the mean ± SD, $^{*}P < 0.05$, $^{**}P < 0.01$, $^{***}P < 0.001$

of compound muscle action potential (CMAP) of the vibrissal muscle, the innervated end target organ, at both the injury and the contralateral healthy sides, were measured at week 12 [42]. The ratio of CMAP of the injured side compared to the normal side was used to evaluate facial nerve functional recovery (Fig. 9c, d). Compared with the nerve conduit alone and GMSC groups, CMAP was significantly restored in the NCSC group with a nearly twofold recovery over these two groups (Fig. 9c).

Histologically, longitudinal sections of the regenerated nerves at the gap defect site in each group were stained with antibodies for S-100β, β-tubulin III, neurofilament, and growth associated protein-43 (GAP-43) for Schwann cell and axonal regeneration. Compared to nerve conduit alone and GMSC groups, Schwann cell and neuronal markers were significantly enhanced in NCSC group (Fig. 10a, b). Meanwhile, the regenerated nerve fibers demonstrated a more highly organized arrangement in the NCSC group as compared with that in nerve conduit alone and GMSC groups (Fig. 10a, b). In addition, the regenerated myelin sheaths were observed by toluidine blue staining (Fig. 9e) and transmission electron microscopy (TEM) (Fig. 9f). The number of myelinated axons, thickness, and G-ratio were evaluated. TEM showed that nerves from implantation of nerve conduit alone group revealed poorly regenerated nerves composed of thin, dispersed myelinated and non-myelinated nerve fibers. In contrast, combinatory implantation of nerve conduit and cells, particularly NCSCs, showed well regenerated nerves composed of thick and ordered myelinated nerve fibers (Fig. 9f). Further analysis showed that the number of myelinated axons and the thickness of the myelin sheaths were significantly higher while the G-ratio was lower in the NCSC group than those in nerve conduit alone and GMSC groups (Fig. 9g–i). These findings suggest that NCSCs exert significantly enhanced potential to facilitate facial nerve regeneration in a rat facial nerve defect model in comparison to the parental GMSCs. Furthermore, the nerve conduit alone may act as a conduit, however, does not substantially regenerate effective facial nerve in this model.

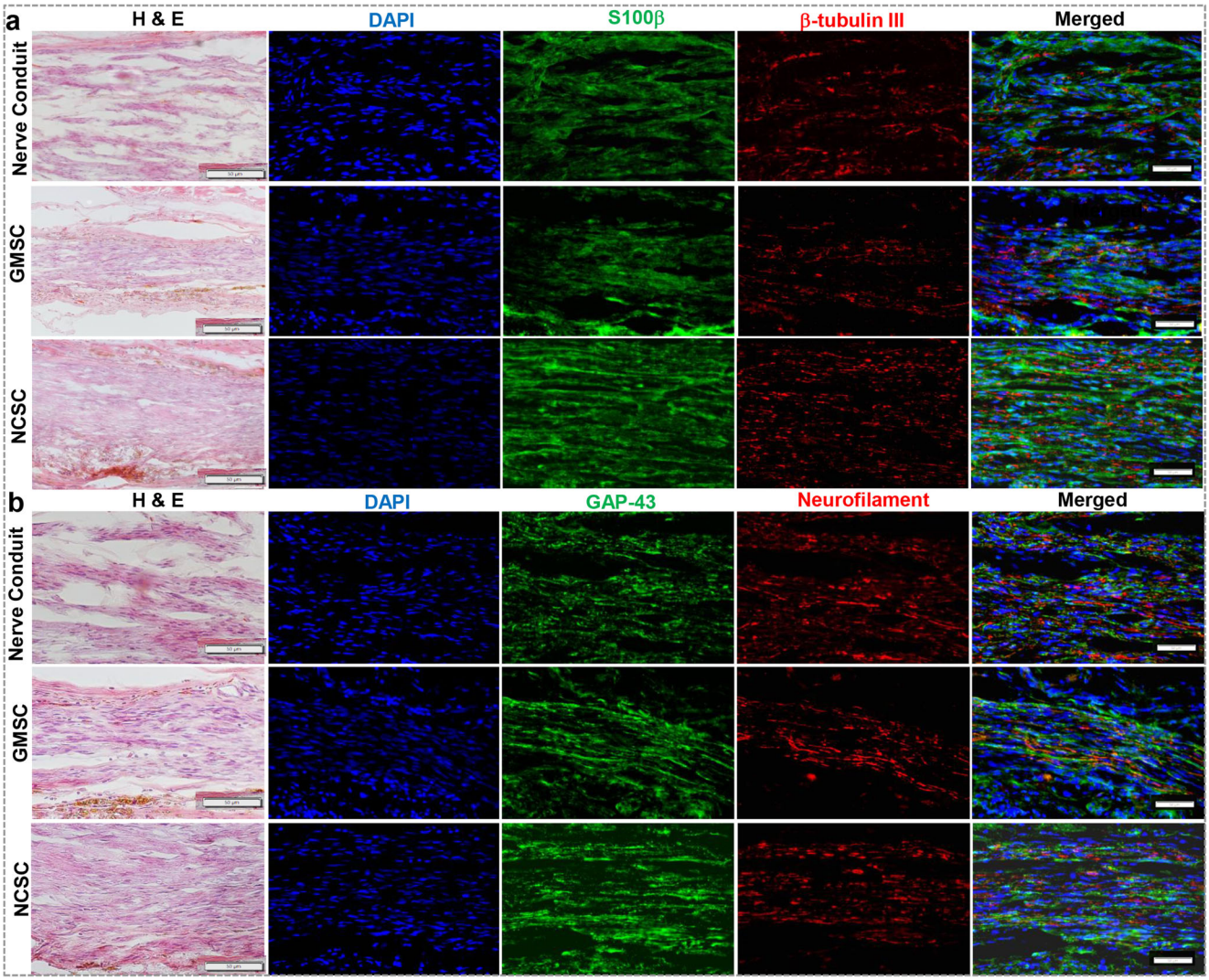

Fig. 10 Histological analysis of regenerated facial nerves. **a** Left panels, H & E staining of cryosections of the middle segment of regenerated facial nerves at 12 weeks after surgery. Scale bars, 200 μm. Immunohistochemistry showed increased expression of S-100β and β-tubulin III, and organized axonal alignment in regenerated nerves from transplantation with NCSC group. Scale bars, 50 μm. **b** Left panels, H & E staining of cryosections of the middle segment of regenerated facial nerves at 12 weeks after surgery. Scale bars, 50 μm. Immunohistochemistry showed increased expression of growth associated protein-43 (GAP-43) and neurofilament, and an organized axonal alignment in regenerated nerves from transplantation with NCSC group. Scale bars, 50 μm. Cell nuclei were counter-stained by DAPI (blue)

Discussion

A variety of adult tissues, such as bone marrow [29, 30], skin [57], hair follicle [58, 59], adipose tissue [30], cornea [60], inferior turbinate [61], and several orofacial tissues [25–27, 62], have been shown to harbor a unique subpopulation of tissue-specific progenitor cells which confer neural crest stem-like cell properties. Even though there is still lack of specific markers to identify and characterize these adult NCSC-like cells due to their heterogeneity and distinct tissue-origins, a panel of NCSC-related genes such as *NESTIN*, $p75^{NTR}$, *SOX9*, *SOX10*, *PAX3*, *FOXD3*, *SNAIL1*, *SLUG*, and *TWIST1* is commonly but differentially expressed in NCSCs [22, 30]. However, among the major NCSC-related transcription factors, *SOX10* has been shown to be consistently expressed in both embryonic and adult NCSCs from rodents [22, 29, 30], but occasionally expressed in NCSCs derived from certain human adult tissues, e.g. hair follicle [59] and inferior turbinate [61]. The lack of SOX10 expression has been reported in adult NCSCs derived from human oral mucosa [25, 27], bone marrow, and adipose tissues [30]. Consistently with these findings, our current study demonstrated that NCSC-like cells induced from human GMSCs under our experimental conditions showed increased protein expressions in NESTIN, $p75^{NTR}$, SOX9, FOXD3, SNAIL1, SLUG, and TWIST1, but not SOX10 (Figs. 1, 2, 3). Even though adult NCSC from different tissues exhibited differences in the expression profile of NCSC-related genes, they

possess similar multipotent differentiation capability into classical NC cell lineages, such as neurons and Schwann cells, and various non-neural cell lineages [22, 30]. Thus, they may represent a promising alternative source of stem cells for cell-based therapy for various human diseases, particularly, for neurological disorders. However, the potential application of these unique tissue-specific NCSCs in tissue engineering/regenerative medicine (TE/RM) is much less frequently investigated in comparison to other types of stem cells and might be hurdled by their scarcity in adult tissues and the difficulty of efficient isolation and ex vivo expansion.

In recent years, direct conversion of somatic cells, e.g., fibroblasts into pluripotent state by reprogramming with a combination of transcription factors or even a single transcription factor is emerging as a novel approach to generate large number of neural stem or progenitor cells for application in TE/RM [12–16, 18, 20]. Most recently, it has been reported that multipotent neural crest cells can be induced by direct reprogramming of human postnatal fibroblasts with enforced expression of a single transcription factor SOX10 [17] or with substrate-mediated transfer of the naked FOXD3 plasmids [31]. Besides gene transfer, other non-genetic approaches such as the use of small molecules, biophysical factors like mechanical properties and substrate topography, have also been used to improve the induction efficiency of NSCs from somatic cells [21, 63]. Suspension or floating sphere culture is a classic approach for isolation and enrichment of neural progenitor cells directly from tissues but the efficiency is relatively low and thus difficult to obtain enough cells within a short time window [22, 47]. Alternatively, two recent studies have reported that human oral mucosa and gingiva-derived MSCs were first expanded in vitro by culture as plastic adherent monolayers in standard serum-containing medium and subsequently subjected to suspension or floating culture with serum-free neural culture medium, which led to a significant enrichment of NCSCs [25, 27]. Herein, we also showed that direct floating sphere-forming culture with serum-free neural culture medium significantly increased the protein expression of several NCSC-related genes, NESTIN, FOXD3, SLUG, SOX9, SNAIL1, and TWIST (Fig. 3). Additionally, it has been shown that changing the mechanical and physical properties of the surface of culture dishes by coating with certain types of materials, e.g., chitosan, promoted adherent human gingival fibroblasts and MSCs to aggregate into spheroids, which showed increased expression of stemness-regulatory genes and the NCSC-related gene SOX9 [64, 65]. In the present study, we showed that subject of human GMSCs ex vivo expanded as adherent monolayers to culturing on laminin (LN)/poly-L-ornithine (PLO)-precoated culture plates under neural induction conditions had stronger inductive effect on the expression of NCSC-related genes and morphological changes than culturing GMSCs on plates pre-coated with either laminin or poly-L-ornithine alone (Fig. 1). However, further studies are warranted to explore whether such stronger inductive effects on the expression of NCSC-related genes mediated by pre-coating with both laminin and poly-L-ornithine involve an elevated expression of extracellular matrix components, particularly the adhesion molecules such as different subtypes of integrin and focal adhesion kinase (FAK), in GMSCs [66].

Geometrical and mechanical signals generated from cell-extracellular matrix (ECM), cell-cell adhesions, the organization of the cytoskeleton and tension forces have added an additional dimension to cell signaling pathways that control cell proliferation, stem cell identity, differentiation, and cell death [50]. However, how mechanical signals are sensed and transduced into the cell nucleus to regulate the downstream gene expressions has long remained largely unknown. Most recently, several lines of evidence have shown that mechanical signals converged on the regulation of the downstream effectors, Yes-associated protein (YAP) and TAZ [50], wherein Rho-associated kinase (ROCK)-mediated non-muscle myosin II (NM II) dependent contraction of the actomyosin cytoskeleton may play an essential role in mechanical signal transduction [54, 55, 67]. Previous studies have shown that Rho/ROCK activity was involved in spheroid formation of human gingival fibroblasts (HGFs) and MSCs upon culturing on chitosan membranes [64, 65]. In the current study, we demonstrated that subjecting GMSCs directly to neurosphere culture or culturing on PLO/LN-precoated plates robustly induced the expression of YAP1, while knockdown of YAP1 expression significantly inhibited the expression of NCSC-related genes (Fig.7). Meanwhile, we further demonstrated that blocking non-muscle myosin II (NMII) and RhoA/Rock activities prevented spheroid formation of GMSCs culturing on LN/PLO-precoated plates and concomitantly inhibited the expression of YAP1 and NCSC-related genes (Fig.8). These compelling findings support the notion that activation of the RhoA-ROCK/YAP1 axis mediated by mechanical cues generated by LN/PLO precoating or neurosphere culture might play an important role in the generation of induced NCSCs from GMSCs. However, further studies are warranted to delineate the overarching signals that orchestrate mechanical cues-mediated generation of NCSCs from GMSCs.

Injuries to peripheral nerves, particularly the facial nerve, often lead to long-term disability, social stigmatization, and decreased function of the end target organs [7]. Currently, autografts of nerves remain as the gold standard approach to bridge the gap between the injured nerve stumps. However, this approach also suffers from several major shortcomings, such as permanent donor site morbidity, limited availability, and the possibility of neuroma formation [7, 68]. In the last several decades, much work has been done to develop a variety of synthetic and natural nerve guidance devices to improve

peripheral nerve regeneration following injuries with small gaps. However, the overall clinical outcomes of these approaches are still disappointing, as yet no suitable replacement for autografts has been developed [7]. Most recently, there has been growing enthusiasm to use stem cells in combination with tissue engineering techniques to promote peripheral nerve regeneration and functional recovery [9]. To date, various types of mesenchymal stem cells or progenitor cells, such as bone marrow mesenchymal stem cells, adipose-derived stem cells, dental pulp stem cells, umbilical MSCs, have been shown to possess certain degrees of beneficial effects on peripheral nerve regeneration [9] due to their multipotent potentials to differentiate into neurons and Schwann cells as well as their ability to produce neurotrophic factors [40, 41, 69–72]. However, the inherent heterogeneity, limited survival abilities, unpredictable cell fate, and the variation of clinical outcomes have significantly impeded their application [7]. In the present study, we demonstrated that transplantation of NCSC-like cells induced from human GMSCs in combination with a nerve conduit, an extracellular matrix coaption aid, exhibited significantly enhanced potentials to facilitate regeneration and functional recovery of rat facial nerve as compared with the parental GMSC counterparts (Figs. 9, 10).

In summary, a small subpopulation of post-migratory neural crest cells (NCCs) is readily accessible from oral and craniofacial tissues, particularly, the easily accessible oral mucosa and gingival tissues. This study presented a simple, safe, and reproducible non-genetic approach to induce ex vivo expanded human GMSCs into NCSCs, whereby the activation of RhoA-ROCK/YAP1 signaling axis triggered by actomyosin cytoskeleton-transduced mechanical cues may play an important role. Functionally, transplantation of GMSC-derived NCSCs in combination with a nerve conduit exhibited significant beneficial effects on rat facial nerve regeneration. These compelling findings suggest that GMSC-derived NCSCs may be a promising and easily accessible stem cell source for generating tissue-engineered nerve constructs that are clinically applicable to improve peripheral nerve regeneration and a potential replacement for the use of autologous nerve grafting.

Author Contributions Qunzhou Zhang: Conception and Design, Collection and/or assembly of data, Data analysis and interpretation, Manuscript writing. Phuong D. Nguyen: Collection and/or assembly of data. Shihong Shi: Collection and/or assembly of data. Justin C. Burrell: Collection and/or assembly of data. Kacy D. Cullen: Conception and Design, Manuscript writing. Anh D. Le: Conception and Design, Manuscript writing, Final approval of manuscript.

Funding Information This work was supported by the National Institute of Health Research Grant, R01DE 019932 (to A. L.), the Osteo Science Foundation (OSF) (to Q. Z. Z., and A. L.), Oral and Maxillofacial Surgery Foundation (OMSF) Research Support Grant (to Q. Z. Z. and A. L.), the Schoenleber Funding Support (A. L.), and the US Department of Defense, W81XWH-16-1-0796 & W81XWH-15-1-0466 (to D. K. C.).

Compliance with Ethical Standards

Conflict of Interest The authors declare that they have no conflict of interest.

References

1. Trounson A, McDonald C (2015) Stem cell therapies in clinical trials: progress and challenges. Cell Stem Cell 17(1):11–22. https://doi.org/10.1016/j.stem.2015.06.007
2. Murphy SV, Atala A (2014) 3D bioprinting of tissues and organs. Nat Biotechnol 32(8):773–785. https://doi.org/10.1038/nbt.2958
3. Mandrycky C, Wang Z, Kim K et al. (2015) 3D bioprinting for engineering complex tissues. Biotechnol Adv
4. Hsieh FY, Hsu SH (2015) 3D bioprinting: a new insight into the therapeutic strategy of neural tissue regeneration. Organogenesis 0
5. Sensharma P, Madhumathi G, Jayant RD, Jaiswal AK (2017) Biomaterials and cells for neural tissue engineering: current choices. Mater Sci Eng C Mater Biol Appl 77:1302–1315. https://doi.org/10.1016/j.msec.2017.03.264
6. Takahashi H, Itoga K, Shimizu T, Yamato M, Okano T (2016) Human neural tissue construct fabrication based on scaffold-free tissue engineering. Adv Healthcare Mater 5(15):1931–1938. https://doi.org/10.1002/adhm.201600197
7. Euler de Souza Lucena E, Guzen FP, Lopes de Paiva Cavalcanti JR, Galvão Barboza CA, Silva do Nascimento Júnior E, Cavalcante JS (2014) Experimental considerations concerning the use of stem cells and tissue engineering for facial nerve regeneration: a systematic review. J Oral Maxillofac Surg 72(5):1001–1012. https://doi.org/10.1016/j.joms.2013.11.006
8. Gu X, Ding F, Williams DF (2014) Neural tissue engineering options for peripheral nerve regeneration. Biomaterials 35(24):6143–6156. https://doi.org/10.1016/j.biomaterials.2014.04.064
9. Bhangra KS, Busuttil F, Phillips JB et al (2016) Using stem cells to grow artificial tissue for peripheral nerve repair. Stem Cells Int 2016:7502178
10. Chambers SM, Fasano CA, Papapetrou EP, Tomishima M, Sadelain M, Studer L (2009) Highly efficient neural conversion of human ES and iPS cells by dual inhibition of SMAD signaling. Nat Biotechnol 27(3):275–280. https://doi.org/10.1038/nbt.1529
11. Picard-Riera N, Nait-Oumesmar B, Baron-Van EA (2004) Endogenous adult neural stem cells: limits and potential to repair the injured central nervous system. J Neurosci Res 76(2):223–231. https://doi.org/10.1002/jnr.20040
12. Kim J, Efe JA, Zhu S, Talantova M, Yuan X, Wang S, Lipton SA, Zhang K et al (2011) Direct reprogramming of mouse fibroblasts to neural progenitors. Proc Natl Acad Sci U S A 108(19):7838–7843. https://doi.org/10.1073/pnas.1103113108
13. Lujan E, Chanda S, Ahlenius H, Sudhof TC, Wernig M (2012) Direct conversion of mouse fibroblasts to self-renewing, tripotent neural precursor cells. Proc Natl Acad Sci U S A 109(7):2527–2532. https://doi.org/10.1073/pnas.1121003109
14. Han DW, Tapia N, Hermann A, Hemmer K, Höing S, Araúzo-Bravo MJ, Zaehres H, Wu G et al (2012) Direct reprogramming of fibroblasts into neural stem cells by defined factors. Cell Stem Cell 10(4):465–472. https://doi.org/10.1016/j.stem.2012.02.021
15. Ring KL, Tong LM, Balestra ME, Javier R, Andrews-Zwilling Y, Li G, Walker D, Zhang WR et al (2012) Direct reprogramming of mouse and human fibroblasts into multipotent neural stem cells with a single factor. Cell Stem Cell 11(1):100–109. https://doi.org/10.1016/j.stem.2012.05.018

16. Thier M, Worsdorfer P, Lakes YB et al (2012) Direct conversion of fibroblasts into stably expandable neural stem cells. Cell Stem Cell 10(4):473–479. https://doi.org/10.1016/j.stem.2012.03.003
17. Kim YJ, Lim H, Li Z, Oh Y, Kovlyagina I, Choi IY, Dong X, Lee G (2014) Generation of multipotent induced neural crest by direct reprogramming of human postnatal fibroblasts with a single transcription factor. Cell Stem Cell 15(4):497–506. https://doi.org/10.1016/j.stem.2014.07.013
18. Yu KR, Shin JH, Kim JJ et al. (2015) Rapid and efficient direct conversion of human adult somatic cells into neural stem cells by HMGA2/let-7b. Cell Rep
19. Su G, Zhao Y, Wei J, Xiao Z, Chen B, Han J, Chen L, Guan J et al (2013) Direct conversion of fibroblasts into neural progenitor-like cells by forced growth into 3D spheres on low attachment surfaces. Biomaterials 34(24):5897–5906. https://doi.org/10.1016/j.biomaterials.2013.04.040
20. Feng N, Han Q, Li J, Wang S, Li H, Yao X, Zhao RC (2014) Generation of highly purified neural stem cells from human adipose-derived mesenchymal stem cells by Sox1 activation. Stem Cells Dev 23(5):515–529. https://doi.org/10.1089/scd.2013.0263
21. Cheng L, Hu W, Qiu B, Zhao J, Yu Y, Guan W, Wang M, Yang W et al (2014) Generation of neural progenitor cells by chemical cocktails and hypoxia. Cell Res 24(6):665–679. https://doi.org/10.1038/cr.2014.32
22. Dupin E, Coelho-Aguiar JM (2013) Isolation and differentiation properties of neural crest stem cells. Cytometry A 83:38–47
23. Kaltschmidt B, Kaltschmidt C, Widera D (2012) Adult craniofacial stem cells: sources and relation to the neural crest. Stem Cell Rev 8(3):658–671. https://doi.org/10.1007/s12015-011-9340-9
24. Boddupally K, Wang G, Chen Y, Kobielak A (2016) Lgr5 marks neural crest derived multipotent oral stromal stem cells. Stem Cells 34(3):720–731. https://doi.org/10.1002/stem.2314
25. Abe S, Yamaguchi S, Sato Y, Harada K (2016) Sphere-derived multipotent progenitor cells obtained from human oral mucosa are enriched in neural crest cells. Stem Cells Transl Med 5(1):117–128. https://doi.org/10.5966/sctm.2015-0111
26. Xu X, Chen C, Akiyama K, Chai Y, AD LE, Wang Z, Shi S (2013) Gingivae contain neural-crest- and mesoderm-derived mesenchymal stem cells. J Dent Res 92(9):825–832. https://doi.org/10.1177/0022034513497961
27. Fournier BP, Loison-Robert LS, Ferre FC et al (2016) Characterisation of human gingival neural crest-derived stem cells in monolayer and neurosphere cultures. Eur Cell Mater 31:40–58. https://doi.org/10.22203/eCM.v031a04
28. Morikawa S, Ouchi T, Shibata S et al (2016) Applications of mesenchymal stem cells and neural crest cells in craniofacial skeletal research. Stem Cells Int 2016:2849879
29. Wislet-Gendebien S, Laudet E, Neirinckx V, Alix P, Leprince P, Glejzer A, Poulet C, Hennuy B et al (2012) Mesenchymal stem cells and neural crest stem cells from adult bone marrow: characterization of their surprising similarities and differences. Cell Mol Life Sci 69(15):2593–2608. https://doi.org/10.1007/s00018-012-0937-1
30. Coste C, Neirinckx V, Sharma A, Agirman G, Rogister B, Foguenne J, Lallemend F, Gothot A et al (2017) Human bone marrow harbors cells with neural crest-associated characteristics like human adipose and dermis tissues. PLoS One 12(7):e0177962. https://doi.org/10.1371/journal.pone.0177962
31. Tseng TC, Hsieh FY, Dai NT, Hsu S (2016) Substrate-mediated reprogramming of human fibroblasts into neural crest stem-like cells and their applications in neural repair. Biomaterials 102:148–161. https://doi.org/10.1016/j.biomaterials.2016.06.020
32. La Noce M, Mele L, Tirino V et al (2014) Neural crest stem cell population in craniomaxillofacial development and tissue repair. Eur Cell Mater 28:348–357. https://doi.org/10.22203/eCM.v028a24
33. Zhang Q, Shi S, Liu Y, Uyanne J, Shi Y, Shi S, AD LE (2009) Mesenchymal stem cells derived from human gingiva are capable of immunomodulatory functions and ameliorate inflammation-related tissue destruction in experimental colitis. J Immunol 183(12):7787–7798. https://doi.org/10.4049/jimmunol.0902318
34. Zhang Q, Nguyen P, Xu Q, Park W, Lee S, Furuhashi A, AD LE (2017) Neural progenitor-like cells induced from human gingiva-derived mesenchymal stem cells regulate myelination of Schwann cells in rat sciatic nerve regeneration. Stem Cells Transl Med 6(2):458–470. https://doi.org/10.5966/sctm.2016-0177
35. Peltier J, Ormerod BK, Schaffer DV (2010) Isolation of adult hippocampal neural progenitors. Methods Mol Biol 621:57–63. https://doi.org/10.1007/978-1-60761-063-2_4
36. Siebzehnrubl FA, Steindler DA (2013) Isolating and culturing of precursor cells from the adult human brain. Methods Mol Biol 1059:79–86. https://doi.org/10.1007/978-1-62703-574-3_7
37. Struckhoff AP, Del Valle L (2013) Neurospheres and glial cell cultures: immunocytochemistry for cell phenotyping. Methods Mol Biol 1078:119–132. https://doi.org/10.1007/978-1-62703-640-5_10
38. Bottenstein JE, Sato GH (1979) Growth of a rat neuroblastoma cell line in serum-free supplemented medium. Proc Natl Acad Sci U S A 76(1):514–517. https://doi.org/10.1073/pnas.76.1.514
39. Barnes D, Sato G (1980) Serum-free cell culture: a unifying approach. Cell 22(3):649–655. https://doi.org/10.1016/0092-8674(80)90540-1
40. Tomita K, Madura T, Sakai Y, Yano K, Terenghi G, Hosokawa K (2013) Glial differentiation of human adipose-derived stem cells: implications for cell-based transplantation therapy. Neuroscience 236:55–65. https://doi.org/10.1016/j.neuroscience.2012.12.066
41. Martens W, Sanen K, Georgiou M, Struys T, Bronckaers A, Ameloot M, Phillips J, Lambrichts I (2014) Human dental pulp stem cells can differentiate into Schwann cells and promote and guide neurite outgrowth in an aligned tissue-engineered collagen construct in vitro. FASEB J 28(4):1634–1643. https://doi.org/10.1096/fj.13-243980
42. Cao J, Xiao Z, Jin W, Chen B, Meng D, Ding W, Han S, Hou X et al (2013) Induction of rat facial nerve regeneration by functional collagen scaffolds. Biomaterials 34(4):1302–1310. https://doi.org/10.1016/j.biomaterials.2012.10.031
43. Sasaki R, Matsumine H, Watanabe Y, Takeuchi Y, Yamato M, Okano T, Miyata M, Ando T (2014) Electrophysiologic and functional evaluations of regenerated facial nerve defects with a tube containing dental pulp cells in rats. Plast Reconstr Surg 134(5):970–978. https://doi.org/10.1097/PRS.0000000000000602
44. Matsumine H, Takeuchi Y, Sasaki R, Kazama T, Kano K, Matsumoto T, Sakurai H, Miyata M et al (2014) Adipocyte-derived and dedifferentiated fat cells promoting facial nerve regeneration in a rat model. Plast Reconstr Surg 134(4):686–697. https://doi.org/10.1097/PRS.0000000000000537
45. Degistirici O, Jaquiery C, Schonebeck B et al (2008) Defining properties of neural crest-derived progenitor cells from the apex of human developing tooth. Tissue Eng A 14(2):317–330. https://doi.org/10.1089/tea.2007.0221
46. Davies LC, Locke M, Webb RD et al (2010) A multipotent neural crest-derived progenitor cell population is resident within the oral mucosa lamina propria. Stem Cells Dev 19(6):819–830. https://doi.org/10.1089/scd.2009.0089
47. Toma JG, McKenzie IA, Bagli D, Miller FD (2005) Isolation and characterization of multipotent skin-derived precursors from human skin. Stem Cells 23(6):727–737. https://doi.org/10.1634/stemcells.2004-0134
48. Nagoshi N, Shibata S, Kubota Y, Nakamura M, Nagai Y, Satoh E, Morikawa S, Okada Y et al (2008) Ontogeny and multipotency of neural crest-derived stem cells in mouse bone marrow, dorsal root ganglia, and whisker pad. Cell Stem Cell 2(4):392–403. https://doi.org/10.1016/j.stem.2008.03.005

49. Menendez L, Yatskievych TA, Antin PB, Dalton S (2011) Wnt signaling and a Smad pathway blockade direct the differentiation of human pluripotent stem cells to multipotent neural crest cells. Proc Natl Acad Sci U S A 108(48):19240–19245. https://doi.org/10.1073/pnas.1113746108
50. Halder G, Dupont S, Piccolo S (2012) Transduction of mechanical and cytoskeletal cues by YAP and TAZ. Nat Rev Mol Cell Biol 13(9):591–600. https://doi.org/10.1038/nrm3416
51. Serinagaoglu Y, Pare J, Giovannini M et al (2015) Nf2-Yap signaling controls the expansion of DRG progenitors and glia during DRG development. Dev Biol 398(1):97–109. https://doi.org/10.1016/j.ydbio.2014.11.017
52. Ding R, Weynans K, Bossing T et al. (2016) The Hippo signalling pathway maintains quiescence in Drosophila neural stem cells. Nat Commun 7
53. Hindley CJ, Condurat AL, Menon V, Thomas R, Azmitia LM, Davis JA, Pruszak J (2016) The hippo pathway member YAP enhances human neural crest cell fate and migration. Sci Rep 6(1):23208. https://doi.org/10.1038/srep23208
54. Yee HF Jr, Melton AC, Tran BN (2001) RhoA/rho-associated kinase mediates fibroblast contractile force generation. Biochem Biophys Res Commun 280(5):1340–1345. https://doi.org/10.1006/bbrc.2001.4291
55. Sandquist JC, Swenson KI, Demali KA et al (2006) Rho kinase differentially regulates phosphorylation of nonmuscle myosin II isoforms A and B during cell rounding and migration. J Biol Chem 281(47):35873–35883. https://doi.org/10.1074/jbc.M605343200
56. Kovacs M, Toth J, Hetenyi C et al (2004) Mechanism of blebbistatin inhibition of myosin II. J Biol Chem 279(34):35557–35563. https://doi.org/10.1074/jbc.M405319200
57. Clewes O, Narytnyk A, Gillinder KR, Loughney AD, Murdoch AP, Sieber-Blum M (2011) Human epidermal neural crest stem cells (hEPI-NCSC)—characterization and directed differentiation into osteocytes and melanocytes. Stem Cell Rev 7(4):799–814. https://doi.org/10.1007/s12015-011-9255-5
58. Biernaskie J (2010) Human hair follicles: "bulging" with neural crest-like stem cells. J Investig Dermatol 130(5):1202–1204. https://doi.org/10.1038/jid.2009.449
59. Krejci E, Grim M (2010) Isolation and characterization of neural crest stem cells from adult human hair follicles. Folia Biol 56(4):149–157
60. Hara S, Hayashi R, Soma T, Kageyama T, Duncan T, Tsujikawa M, Nishida K (2014) Identification and potential application of human corneal endothelial progenitor cells. Stem Cells Dev 23(18):2190–2201. https://doi.org/10.1089/scd.2013.0387
61. Hauser S, Widera D, Qunneis F, Müller J, Zander C, Greiner J, Strauss C, Lüningschrör P et al (2012) Isolation of novel multipotent neural crest-derived stem cells from adult human inferior turbinate. Stem Cells Dev 21(5):742–756. https://doi.org/10.1089/scd.2011.0419
62. Pelaez D, Huang CY, Cheung HS (2013) Isolation of pluripotent neural crest-derived stem cells from adult human tissues by connexin-43 enrichment. Stem Cells Dev 22(21):2906–2914. https://doi.org/10.1089/scd.2013.0090
63. Yoo J, Noh M, Kim H, Jeon NL, Kim BS, Kim J (2015) Nanogrooved substrate promotes direct lineage reprogramming of fibroblasts to functional induced dopaminergic neurons. Biomaterials 45:36–45. https://doi.org/10.1016/j.biomaterials.2014.12.049
64. Hsu SH, Huang GS, Lin SY et al (2012) Enhanced chondrogenic differentiation potential of human gingival fibroblasts by spheroid formation on chitosan membranes. Tissue Eng A 18(1-2):67–79. https://doi.org/10.1089/ten.tea.2011.0157
65. Huang GS, Dai LG, Yen BL, Hsu S (2011) Spheroid formation of mesenchymal stem cells on chitosan and chitosan-hyaluronan membranes. Biomaterials 32(29):6929–6945. https://doi.org/10.1016/j.biomaterials.2011.05.092
66. Boyle ST, Samuel MS (2016) Mechano-reciprocity is maintained between physiological boundaries by tuning signal flux through the Rho-associated protein kinase. Small GTPases 7(3):139–146. https://doi.org/10.1080/21541248.2016.1173771
67. Calvo F, Ege N, Grande-Garcia A, Hooper S, Jenkins RP, Chaudhry SI, Harrington K, Williamson P et al (2013) Mechanotransduction and YAP-dependent matrix remodelling is required for the generation and maintenance of cancer-associated fibroblasts. Nat Cell Biol 15(6):637–646. https://doi.org/10.1038/ncb2756
68. Volk GF, Pantel M, Guntinas-Lichius O (2010) Modern concepts in facial nerve reconstruction. Head Face Med 6(1):25. https://doi.org/10.1186/1746-160X-6-25
69. Kingham PJ, Kolar MK, Novikova LN, Novikov LN, Wiberg M (2014) Stimulating the neurotrophic and angiogenic properties of human adipose-derived stem cells enhances nerve repair. Stem Cells Dev 23(7):741–754. https://doi.org/10.1089/scd.2013.0396
70. Guo ZY, Sun X, Xu XL, Zhao Q, Peng J, Wang Y (2015) Human umbilical cord mesenchymal stem cells promote peripheral nerve repair via paracrine mechanisms. Neural Regen Res 10(4):651–658. https://doi.org/10.4103/1673-5374.155442
71. Gervois P, Struys T, Hilkens P, Bronckaers A, Ratajczak J, Politis C, Brône B, Lambrichts I et al (2015) Neurogenic maturation of human dental pulp stem cells following neurosphere generation induces morphological and electrophysiological characteristics of functional neurons. Stem Cells Dev 24(3):296–311. https://doi.org/10.1089/scd.2014.0117
72. Yamamoto T, Osako Y, Ito M et al. (2015) Trophic effects of dental pulp stem cells on Schwann Cells in peripheral nerve regeneration. cell transplantation